



**Transpiration from subarctic deciduous woodlands:
environmental controls and contribution to ecosystem
evapotranspiration**

Journal:	<i>Ecohydrology</i>
Manuscript ID	ECO-19-0070.R1
Wiley - Manuscript type:	Research Article
Date Submitted by the Author:	10-Nov-2019
Complete List of Authors:	Sabater, Ana Maria; Universitat Autònoma de Barcelona; CREAM; University of Alicante; CEAM Ward, Helen; University of Innsbruck, Department of Atmospheric and Cryospheric Sciences Hill, Tim; University of Exeter, Department of Geography Gornall, Jemma; Met Office Wade, Thomas; The University of Edinburgh Evans, Jonathan; Centre for Ecology and Hydrology Prieto-Blanco, Ana; UCL Disney, Mathias; UCL; NCEO Phoenix, Gareth; The University of Sheffield Williams, Mathew; The University of Edinburgh Huntley, Brian; Durham University Baxter, Robert; Durham University Mencuccini, Maurizio; ICREA; CREAM Poyatos, Rafael; CREAM; Universitat Autònoma de Barcelona; Ghent University
Keywords:	Arctic, branch cuvettes, eddy covariance, evapotranspiration partitioning, mountain birch, tundra, understorey, boreal forest

SCHOLARONE™
Manuscripts

1
2
3 **1 Transpiration from subarctic deciduous woodlands: environmental controls and**
4 **2 contribution to ecosystem evapotranspiration.**

3 Ana M. Sabater ^{1,2,3,4}, Helen C. Ward ⁵, Timothy C. Hill ⁶, Jemma L. Gornall⁷, Thomas
4 J. Wade ⁸, Jonathan G. Evans ⁹, Ana Prieto-Blanco ¹⁰, Mathias Disney ^{10, 11}, Gareth K.
5 Phoenix ¹², Mathew Williams ⁸, Brian Huntley ¹³, Robert Baxter ¹³, Maurizio
6 Mencuccini ^{2, 14}, Rafael Poyatos ^{1, 2, 15}

7
8 ¹ Universitat Autònoma de Barcelona, Barcelona, Spain.

9 ² CREAM, Cerdanyola del Vallès, Barcelona, Spain.

10 ³ Fundación CEAM, Joint Research Unit University of Alicante-CEAM, Alicante,
11 Spain.

12 ⁴ Department of Ecology, University of Alicante, Alicante, Spain.

13 ⁵ Department of Atmospheric and Cryospheric Sciences (ACINN), University of
14 Innsbruck, Innsbruck, Austria.

15 ⁶ College of Life and Environmental Sciences, Department of Geography, University of
16 Exeter, Exeter, UK.

17 ⁷ Met Office, Exeter, UK.

18 ⁸ School of Geosciences, University of Edinburgh, Edinburgh, UK.

19 ⁹ Centre for Ecology and Hydrology, Wallingford, UK.

20 ¹⁰ University College London, Department of Geography, London, UK.

21 ¹¹ NERC National Centre for Earth Observation (NCEO), Leicester, UK.

22 ¹² Department of Animal and Plant Sciences, University of Sheffield, Sheffield, UK.

23 ¹³ Department of Biosciences, Durham University, Durham, UK.

24 ¹⁴ ICREA, Barcelona, Spain.

25 ¹⁵ Laboratory of Plant Ecology, Faculty of Bioscience Engineering, Ghent University,
26 Ghent, Belgium.

27 Correspondence. R. Poyatos, CREAM, Edifici C, Campus UAB Bellaterra, E08193
28 Barcelona, Spain. Email: r.poyatos@creaf.uab.es, Tel.+34 935814676, Fax:
29 +34935814151.

30 Short title: Transpiration and evapotranspiration of subarctic deciduous woodlands

1
2
3 **31 Abstract**
4

5
6 32 Potential land-climate feedbacks in subarctic regions, where rapid warming is driving
7
8 33 forest expansion into the tundra, may be mediated by differences in transpiration of
9
10 34 different plant functional types. Here we assess the environmental controls of overstorey
11
12 35 transpiration and its relevance for ecosystem evapotranspiration in subarctic deciduous
13
14 36 woodlands. We measured overstorey transpiration of mountain birch canopies and
15
16 37 ecosystem evapotranspiration in two locations in northern Fennoscandia, having dense
17
18 38 (Abisko) and sparse (Kevo) overstories. For Kevo, we also upscale chamber-measured
19
20 39 understorey evapotranspiration from shrubs and lichen using a detailed land cover map.
21
22 40 Sub-daily evaporative fluxes were not affected by soil moisture, and showed similar
23
24 41 controls by vapour pressure deficit and radiation across sites. At the daily timescale,
25
26 42 increases in evaporative demand led to proportionally higher contributions of overstorey
27
28 43 transpiration to ecosystem evapotranspiration. For the entire growing season, the
29
30 44 overstorey transpired 33% of ecosystem evapotranspiration in Abisko and only 16% in
31
32 45 Kevo. At this latter site, the understorey had a higher leaf area index and contributed
33
34 46 more to ecosystem evapotranspiration compared to the overstorey birch canopy. In
35
36 47 Abisko, growing season evapotranspiration was 27% higher than precipitation,
37
38 48 consistent with a gradual soil moisture depletion over the summer. Our results show that
39
40 49 overstorey canopy transpiration in subarctic deciduous woodlands is not the dominant
41
42 50 evaporative flux. However, given the observed environmental sensitivity of
43
44 51 evapotranspiration components, the role of deciduous trees in driving ecosystem
45
46 52 evapotranspiration may increase with the predicted increases in tree cover and
47
48 53 evaporative demand across subarctic regions.
49

50
51
52
53
54 **54 Keywords**
55

56 Arctic, branch cuvettes, eddy covariance, evapotranspiration partitioning, mountain
57
58 birch, tundra, understorey
59

60
57

58 **Introduction**

59 Northern high latitudes (boreal and arctic biomes) exert an important influence in global
60 biosphere-atmosphere interactions involving water, energy and atmospheric
61 composition. These interactions are globally relevant because of the large extent of
62 these biomes (arctic tundra and boreal forest cover *ca.* $1.24 \cdot 10^8$ km²) and the intense
63 and rapid warming occurring at northern high latitudes (0.5 K/decade since 1979; IPCC,
64 2013), which is partly driven by regional positive feedbacks (Chapin et al., 2000).
65 Warmer temperatures and longer growing seasons are already inducing poleward and
66 altitudinal treeline migration and shrub expansion in the tundra zone, which may in turn
67 drive considerable land-atmosphere feedbacks in these latitudes (Kattsov et al., 2005;
68 Swann, Fung, Levis, Bonan, & Doney, 2010; Zhang et al., 2013)

69 Treelines across the subarctic vegetation belt are largely dominated by conifers,
70 although deciduous broadleaves occupy 18% of the forest area at latitudes above 60°
71 across Eurasia (Krankina et al., 2010) and can form the tundra-to-forest transition in
72 many subarctic regions with oceanic influence (Callaghan et al., 2005). The area of
73 deciduous broadleaf woodlands is increasing throughout the subarctic region (Hofgaard,
74 Tømmervik, Rees, & Hanssen, 2013; Rundqvist et al., 2011; Tømmervik et al., 2004;
75 Wang et al., 2019), following a general trend of increasing deciduous vegetation at
76 northern high latitudes (Myers-Smith et al., 2011). These vegetation changes are
77 predicted to continue in the future (Mekonnen, Riley, Randerson, Grant, & Rogers,
78 2019) and may cause substantial land-climate feedbacks mediated by changes in albedo,
79 in carbon sequestration and in evaporative fluxes (Bonan, 2008; Bonfils et al., 2012).
80 Higher transpiration rates by deciduous broadleaf forests could lead to stronger
81 evaporative cooling locally (Chapin et al., 2000), although, in a regional context, the
82 effects of the expansion of deciduous broadleaf trees into the tundra zone can be more
83 complex and actually enhance Arctic warming (Swann et al., 2010). Moreover,
84 increased soil moisture uptake by deciduous trees could lead to faster depletion of
85 snowmelt water during the shoulder season, triggering further hydrological changes
86 (Young-Robertson, Bolton, Bhatt, Cristóbal, & Thoman, 2016). Therefore, a greater
87 understanding of the magnitudes and controls of evapotranspiration in deciduous
88 woodlands is needed to predict future changes in land-atmosphere interactions in
89 subarctic forest-tundra ecotones.

1
2
3 90 Syntheses addressing magnitudes and drivers of ecosystem evapotranspiration (ET_{eco}) at
4
5 91 northern high latitudes show a paucity of data for deciduous broadleaf forests from
6
7 92 subarctic locations (Brümmer et al., 2011; Kasurinen et al., 2014; McFadden, Eugster,
8
9 93 & Chapin III, 2003). These syntheses show that leaf area index (LAI), meteorological
10
11 94 conditions and physiological regulation by vegetation are the three major factors
12
13 95 affecting ET_{eco} in northern high-latitude ecosystems. In these ecosystems,
14
15 96 evapotranspiration is largely driven by vapour pressure deficit (VPD), radiation and
16
17 97 temperature, with soil moisture often playing a minor role (Beringer, Chapin,
18
19 98 Thompson, & McGuire, 2005; Brümmer et al., 2011). In deciduous forests, growing
20
21 99 season duration also affects seasonal evapotranspiration through the influence on LAI
22
23 100 phenology (Brümmer et al., 2012). Deciduous broadleaf forests from northern high
24
25 101 latitudes show higher evapotranspiration rates compared to conifer forests in the same
26
27 102 region (Brümmer et al., 2011; Kasurinen et al., 2014), but they may also display a
28
29 103 stronger stomatal control with increasing VPD (Welp, Randerson, & Liu, 2007).
30
31 104 However, to what extent do these patterns in the drivers of ET_{eco} from northern high-
32
33 105 latitude deciduous forests reflect the transpiration regulation by the main canopy?

34
35 106 The partitioning of ET_{eco} into transpiration and evaporation and the factors controlling
36
37 107 this partitioning are still poorly known (Schlesinger & Jasechko, 2014). Subarctic and
38
39 108 northern boreal woodlands typically show a low LAI of the dominant canopy species,
40
41 109 meaning that the contribution of understorey and soil evaporation to ecosystem
42
43 110 evapotranspiration may be moderate to high (Blanken et al., 2001; Iida et al., 2009;
44
45 111 Lafleur, 1992), although it will depend on vegetation structure (Beringer et al., 2005).
46
47 112 This substantial contribution of the soil and understorey to ET_{eco} implies that eddy flux-
48
49 113 based estimates of ET_{eco} in these forests may well represent the mix of physical and
50
51 114 biological controls on evaporative fluxes and will only partially capture the
52
53 115 physiological regulation exerted by the main canopy (Ikawa et al., 2015; Kasurinen et
54
55 116 al., 2014). Evaporative fluxes of overstorey, understorey and the forest floor may have
56
57 117 contrasting hydroclimatic responses (Iida et al., 2009) and a strong seasonal variation
58
59 118 (Blanken et al., 2001). Although several studies have addressed the magnitudes and
60
119 drivers of the different components of ET_{eco} in northern boreal and subarctic forests
120 (Blanken et al., 2001; Grelle, Lundberg, Lindroth, Morén, & Cienciala, 1997; Iida et al.,

1
2
3 121 2009; Ikawa et al., 2015), we are not aware of any study of these characteristics from
4
5 122 subarctic deciduous woodlands.

6
7 123 In this article, we quantify the magnitude and seasonal controls on ET_{eco} and on the
8
9 124 transpiration of the main canopy in two deciduous broadleaf woodlands dominated by
10
11 125 mountain birch (*Betula pubescens* ssp. *czerepanovii* (Orlova) Hamet- Ahti). This is a
12
13 126 representative species of subarctic woodlands covering 600000 ha throughout northern
14
15 127 Fennoscandia (Haapanala et al., 2009). The Abisko site (N Sweden) displays a denser
16
17 128 birch woodland compared to the sparser Kevo site (N Finland), which is also slightly
18
19 129 colder and wetter. Therefore, the Abisko woodland would be representative of denser
20
21 130 canopies which are becoming common across the subarctic in response to warming and
22
23 131 reduced browsing (Callaghan et al., 2013). In both sites, we measured ET_{eco} and birch
24
25 132 transpiration per leaf area (T_{leaf}), which was upscaled to the birch canopy level (T_{birch}).
26
27 133 Our main goals were: (1) to identify the drivers of ET_{eco} and T_{leaf} , to understand the
28
29 134 environmental controls between the two scales (ecosystem vs branch) and at sites,
30
31 135 which differed substantially in stand structure (denser in Abisko, sparser in Kevo); and
32
33 136 (2) to investigate how variation in canopy structure affects growing season values of
34
35 137 ET_{eco} relative to growing season precipitation and to quantify the contribution of T_{birch}
36
37 138 to ET_{eco} . To further understand this evapotranspiration partitioning in subarctic
38
39 139 deciduous woodlands, at Kevo we also upscaled evaporative fluxes from birch and
40
41 140 understorey ($ET_{upscaled}$) to explore how this variable compares to ET_{eco} .

42

43 142 **2. Methodology**

44 143 *2.1. Study sites*

45
46 144 Two mountain birch (*Betula pubescens* ssp. *czerepanovii*) forest sites within the
47
48 145 northern Fennoscandia sub-Artic vegetation belt were chosen for this study: Abisko
49
50 146 (northern Sweden) and Kevo (northern Finland). Both sites were located near the
51
52 147 mountain birch/tundra ecotone, where mountain birches are polycormic because of the
53
54 148 harsh environmental conditions and the frequent defoliation by autumn and winter
55
56 149 moths (*Epirrita autumnata* and *Operophtera brumata*). At both sites, we measured
57
58 150 transpiration of mountain birch branches, ecosystem evapotranspiration and other

1
2
3 151 environmental drivers during the mountain birch leaf-on period, hereby abbreviated as
4 152 'growing season', of 2007 (Abisko, DOY 153-241) and of 2008 (Kevo, DOY 171-257).

5
6
7 153 In Abisko (Figure 1a), measurements were undertaken at a location (68.326°N,
8 154 18.833°E, 519 m.a.s.l.) ca. 3.2 km south-east of the Abisko Research Station. At the
9 155 study site, mean annual temperature is -0.9°C and mean annual precipitation is 335 mm
10 156 (1980-2010, temperature corrected assuming a lapse rate of 0.55 °C per 100 m of
11 157 elevation). The predominant substrate is coarse glacial till and soils are typically micro-
12 158 podzols, with no permafrost present (Hartley, Hopkins, Sommerkorn, & Wookey,
13 159 2010). The landscape presents a relatively complex topography, which results in highly
14 160 variable forest cover (Nyström, Holmgren, & Olsson, 2012) and stand structures (Table
15 161 1). Understorey vegetation is dominated by the dwarf shrubs *Empetrum nigrum* ssp
16 162 *hermaphroditum*, *Vaccinium myrtillus* and *Vaccinium uliginosum* (Hartley et al., 2010;
17 163 Poyatos, Gornall, Mencuccini, Huntley, & Baxter, 2012).

18
19
20
21
22
23
24
25
26
27 164 In Kevo (Figure 1b), measurements were undertaken at a location (69.492°N, 27.234°E,
28 165 260 m.a.s.l.) ca. 40 km south of the Kevo Subarctic Research Institute. Climate at the site
29 166 (1978-2007, data from the the Kevo Institute station, corrected for lapse rate) is colder
30 167 and wetter than in Abisko (-2.4°C and 422 mm mean annual temperature and
31 168 precipitation, respectively) and the substrate is composed of gneiss covered by glacial
32 169 till, and no permafrost is present at the forest site. Mountain birch forests in Kevo,
33 170 located upon gentle slopes/ridges and surrounded by mires in topographically depressed
34 171 areas, were sparser and showed a more homogeneous structure compared to Abisko
35 172 (Table 1). Understorey vegetation showed a higher LAI compared to Abisko (Table 1);
36 173 it consisted of *E. nigrum* below mountain birch canopies and distinct patches covered
37 174 by *Betula nana* L. and *Cladonia* spp, lichens in the open areas (Poyatos et al., 2012).

38
39
40
41
42
43
44
45
46
47 175

48
49 176 One forest inventory was established in the vicinity of each of the branch bags sites to
50 177 quantify stand structure at the plot level (a 10-m circular plot in Abisko and a 30 x 30 m
51 178 plot in Kevo). Another set of 30 x 30 m plots was measured in Abisko (N = 5) and Kevo
52 179 (N = 7) to quantify ecosystem-level stand structure and maximum leaf area index,
53 180 LAI_{max} (m² leaf m⁻²ground). Forest inventory plots were at an average distance from the
54 181 eddy flux tower of 105 m in Abisko and 450 m in Kevo. Diameters and heights of all

1
2
3 182 stems with diameter at breast height $DBH > 12$ mm within the plots were measured in
4 183 2007 at Abisko and in 2008 at Kevo. For Abisko, we used published allometric
5 184 equations predicting leaf biomass from stem basal area and height (Dahlberg, Berge,
6 185 Petersson, & Vencatasawmy, 2004) to convert leaf biomass supported by each stem into
7 186 leaf area using site-specific leaf mass per area. For Kevo, we harvested $N = 15$ stems
8 187 during the peak growing season in 2008, to measure their leaf area and we obtained site-
9 188 specific allometries between stem diameter and leaf area (Table S1). Understorey
10 189 LAI_{max} was obtained from 1 m² vegetation surveys ($N = 5$) in each of the sites,
11 190 following Fletcher et al. (2012).

191 2.2. Branch-level transpiration measurements

192 At both sites, we selected eight mountain birch branches representative of low and mid-
193 canopy conditions for branch transpiration measurements. Branch transpiration was
194 measured using a multiplexed branch bag device based on the closed system approach
195 (Rayment & Jarvis, 1999; Wingate, Seibt, Moncrieff, Jarvis, & Lloyd, 2007). This
196 system measures water vapour concentration changes within eight 0.11 m³ ventilated
197 cuvettes enclosing individual branches during 7.5 minutes. Branches were measured
198 sequentially, and a measurement cycle of all eight branches was completed within an
199 hour. During each measurement period, air temperature, T (°C), relative humidity, RH
200 (%), and photosynthetically active radiation, PAR ($\mu\text{mol photons m}^{-2} \text{ s}^{-1}$), were
201 recorded every 5 seconds by a datalogger. The system also recorded the value of
202 environmental variables at the beginning of each transpiration observation (i.e. hourly).
203 The subscript 'branch' was used to refer to branch-level meteorological variables
204 (PAR_{branch} , VPD_{branch}). Further technical details of the branch bags system and of the
205 calculation of branch-level transpiration can be found in the Supporting Information S2.

206 We quantified branch transpiration on a leaf area basis, T_{leaf} ($l \text{ m}^{-2} \text{ hour}^{-1}$), by dividing
207 whole-branch transpiration by the leaf area of the branch within the bag. To account for
208 seasonal variation in branch leaf area, we periodically counted the number of leaves
209 inside the bags during the growing season. We then multiplied the leaf counts by an
210 estimation of the average leaf area obtained from a sample of leaves ($N = 10$) close to
211 the measured branch, fitted a nonlinear response as a function of day of year and, if
212 needed, corrected by differences in leaf size between inside and outside the bags

1
2
3 213 (Poyatos et al., 2012). We expressed the seasonal variation in leaf area in relative terms
4 214 between 0 and 1 (minimum and maximum leaf area, respectively) to use for the
5 215 upscaling of branch transpiration fluxes.
6
7

8 9 216 *2.3. Ecosystem evapotranspiration and environmental monitoring*

10
11 217 At both sites, half-hourly ecosystem evapotranspiration, ET_{eco} (mm h⁻¹), was estimated
12 218 from latent heat measurements using the eddy covariance (EC) technique in flux towers
13 219 located above the mountain birch canopy (Aubinet, Vesala, & Papale, 2012). The three
14 220 components of wind speed were measured with a sonic anemometer (R3, Gill
15 221 Instruments, Lymington, UK) and water vapour concentrations were measured by an
16 222 open-path infrared gas analyser (LI-7500, LI-COR Biosciences, Lincoln, USA). Raw
17 223 data were logged at 20 Hz and processed to 30-minute statistics using FluxView (Centre
18 224 for Ecology and Hydrology, Wallingford, UK) and quality-controlled following
19 225 standard procedures. These include correcting sonic data for angle-of-attack (Gash &
20 226 Dolman, 2003), compensating for the lag time between sonic and gas analyser, rotating
21 227 the co-ordinate system (so that the horizontal wind vector is aligned with the 30-min
22 228 mean and the vertical component is forced to zero), correcting sonic temperature for
23 229 humidity (Schotanus, Nieuwstadt, & De Bruin, 1983), correcting the fluxes for high-
24 230 and low- frequency spectral losses and correcting gas fluxes for density effects (Webb,
25 231 Pearman, & Leuning, 1980). Quality control involved despiking and removal of data
26 232 outside physically reasonable limits, when instruments malfunctioned, when the
27 233 windows of the gas analyser were wet or dirty, and during periods of heavy rain.
28 234 Filtering of data during low turbulence conditions based on a friction velocity threshold
29 235 was not applied. Energy balance closure was within the expected range (Stoy et al.,
30 236 2013) and did not differ much across sites (Supplementary Information S3).
31
32
33
34
35
36
37
38
39
40
41
42
43
44
45

46 237 Meteorological stations installed at the flux towers measured half-hourly values of
47 238 temperature, relative humidity, PAR and precipitation above the birch canopy and we
48 239 refer to them using the subscript 'eco' (PAR_{eco} , VPD_{eco}). Soil volumetric water content
49 240 in the upper 30 cm of the soil, SWC (cm³ cm⁻³), was measured with 1 or 2 frequency
50 241 domain reflectometers (CS616, Campbell Scientific, UK) at each site. To account for
51 242 site-specific differences in maximum and minimum water-holding capacity, we
52
53
54
55
56
57
58
59
60

1
2
3 243 transformed SWC into soil moisture deficit (SMD), which ranged from 0 (maximum
4 soil moisture) to 1 (minimum soil moisture) (Granier & Loustau, 1994).

7 245 2.4. Modelling environmental controls of evaporative fluxes

9 246 Firstly, T_{leaf} and ET_{eco} data were filtered ($PAR > 50 \mu\text{mol photons m}^{-2} \text{ s}^{-1}$) to avoid noisy
11 vapour concentration data in the branch bags and low turbulence conditions in the case
12 of EC. For T_{leaf} , the values of the meteorological drivers were measured locally in each
13 individual branch (VPD_{branch} , PAR_{branch}) and for ET_{eco} they were measured above the
14 canopy (VPD_{eco} , PAR_{eco}).
15
16
17
18

19 251 All models were fitted using the nlme package (Pinheiro, Bates, DebRoy, Sarkar, & R
20 Core Team, 2018) in R (R Core Team 2016). T_{leaf} was modelled using a linear mixed
21 effects model (lme), with VPD_{branch} , PAR_{branch} and SMD as fixed factors and ET_{eco} was
22 fitted as a function of VPD_{eco} , PAR_{eco} and SMD using a generalized least squares model
23 (gls). In view of the residual distributions after preliminary analyses, we log-
24 transformed the response variables, T_{leaf} and ET_{eco} , and the explanatory variables, except
25 for the case of PAR in ET_{eco} modelling. All models included a first-order autoregressive
26 correlation structure for the residuals, specifying fractional day of year as a continuous
27 time covariate. We applied model selection to include those terms which minimised the
28 value of the Akaike Information Criterion (AIC) while checking that variance inflation
29 factors were below 10 (Zuur, Ieno, & Elphick, 2010). Model selection was carried out
30 with models fitted using maximum likelihood, but final models were fitted using
31 restricted maximum likelihood (Pinheiro & Bates, 2000). Normality, linearity and
32 homoscedasticity of residuals were visually inspected and temporal autocorrelation was
33 analysed visually by autocorrelation plots using the *acf* function in R. We calculated
34 marginal and conditional R^2 , the proportion of variance explained by fixed and by both
35 fixed and random factors, respectively (Nakagawa & Schielzeth, 2013).
36
37
38
39
40
41
42
43
44
45
46
47
48

49 268 2.5. Overstorey contributions to ecosystem evapotranspiration

51 269 Before upscaling, evaporative flux data were aggregated at the daily scale, using models
52 obtained in section 2.4 to gap-fill missing hourly data and fitting daily models when
53 meteorological data from the measurement systems were missing (Supporting
54 Information S4). We obtained transpiration of the mountain birch canopy, T_{birch} (mm
55 day⁻¹), by multiplying T_{leaf} by the LAI of mountain birch in each stand (Table 1),
56
57
58
59
60

1
2
3 274 corrected for seasonal variation (see section 2.2). The calculation was done using mean
4
5 275 and \pm standard error (SE) of the LAI values, to propagate the uncertainty of the LAI
6
7 276 values at each site into the upscaled estimates of T_{birch} .

8
9 277 At both sites we calculated the mountain birch contribution to daily ecosystem
10
11 278 evapotranspiration, T_{birch}/ET_{eco} (%). We analysed T_{birch}/ET_{eco} as a separate linear model
12
13 279 of VPD, PAR (both log-transformed) and SMD, including a factor coding for site
14
15 280 (Abisko and Kevo) which interacted with each of the environmental drivers. Model
16
17 281 selection was carried out based on AIC, as described in section 2.4. We also tested for a
18
19 282 possible influence of interception and subsequent canopy evaporation on T_{birch}/ET_{eco} by
20
21 283 testing for differences between dry and wet days, using a gls model as described in the
22
23 284 previous paragraph. We considered wet days as those within 2 days after a precipitation
24
25 285 event > 1 mm, assuming all wet surfaces would have dried up during this period
26
27 286 (Knauer, Werner, & Zaehle, 2015).

28
29 287 Growing season values (mm) of precipitation (P), T_{birch} , ET_{eco} and $ET_{upscaled}$ were
30
31 288 calculated by aggregating daily values. We also quantified the overall growing season
32
33 289 contribution of T_{birch} and $ET_{upscaled}$ to ET_{eco} and expressed growing season evaporative
34
35 290 fluxes as a percentage of growing season precipitation.

36 291 2.6. Upscaling evapotranspiration components in Kevo

37 292 In Kevo, measurements of evapotranspiration were available for other ecosystem
38
39 293 components, i.e., understory shrubs and lichen (Table S3, Figure 1). These
40
41 294 evapotranspiration measurements were representative of small patches and were
42
43 295 obtained with an automated chamber system (Poyatos et al., 2014) operated during the
44
45 296 2008 growing season, in a forest-mire ecotone ca. 200 m from the flux tower (Figure 1).
46
47 297 Hourly evapotranspiration of 12 tundra plots was calculated similarly to branch bags
48
49 298 fluxes (Supporting Information S5). Because of microclimatic alterations, water vapour
50
51 299 sorption in the tubing system and imperfect chamber sealing the automated chamber
52
53 300 system used here has been reported to underestimate the evaporative fluxes (Cohen et
54
55 301 al., 2015). Therefore, we applied a correction factor of 2.3, obtained in that study, which
56
57 302 used a similar device under comparable environmental conditions (Cohen et al., 2015).

58 303 Shrub evapotranspiration (ET_{shrub}) was estimated as the mean of $N = 9$ plots (mean
59
60 304 $LAI_{max} \pm SE = 0.77 \pm 0.2$) with dwarf tundra vegetation (mainly *Empetrum*

305 *hermaphroditum*, *Calluna vulgaris* and *Vaccinium* spp.) while lichen evaporation
 306 (ET_{lichen}) was calculated as the mean of $N = 3$ lichen heath plots (Poyatos et al., 2014).
 307 We then combined evapotranspiration of the individual components with the fractional
 308 covers (f) of each component within the footprint of the flux tower. Fractional covers
 309 were obtained from aerial photography obtained in August 2008 and subsequent
 310 vegetation classification (Hartley et al., 2015). We used a dynamic footprint approach
 311 (Hartley et al., 2015) to obtain f values which varied with atmospheric conditions,
 312 although results were comparable to those using a simpler, fixed footprint approach
 313 (Figure S4). We calculated $ET_{upscaled}$ (mm day^{-1}) as the product of the time-variable f of
 314 each component and its corresponding T or ET value:

$$315 \quad ET_{upscaled} = T_{birch} + f_{birch} \cdot ET_{shrub} + f_{shrub} \cdot ET_{shrub} + f_{lichen} \cdot ET_{lichen} \quad (1)$$

316 Where f_{birch} , f_{shrub} and f_{lichen} represent the fractional covers of birch forest, understory
 317 shrubs and lichen, respectively. This equation assumes that shrubs were also typically
 318 present under the birch canopies (cf. section 2.1) and that components other than birch,
 319 shrubs and lichen (around 5% of fractional cover, Table S3) behave similarly to shrubs.

321 3. Results

322 3.1. Temporal variation of environmental variables and evaporative fluxes

323 Evaporative demand (Figure 2a-d) was higher in Abisko than in Kevo, as shown by
 324 higher mean growing season values (\pm standard deviation, SD) of air temperatures (10.5
 325 $^{\circ}\text{C} \pm 3.8$ and $9.5^{\circ}\text{C} \pm 3.6$, respectively), VPD_{eco} (0.5 ± 0.3 kPa and 0.3 ± 0.2 kPa) and
 326 PAR_{eco} (407.0 ± 170.0 $\mu\text{mol m}^{-2} \text{s}^{-1}$ and 260.4 ± 130.3 $\mu\text{mol m}^{-2} \text{s}^{-1}$). Light transmission
 327 through the birch canopy was higher in Kevo: PAR_{branch}/PAR_{eco} was 56% in Kevo
 328 compared to 30% in Abisko (Figure 2a,b). This was associated with the larger
 329 difference between VPD_{branch} and VPD_{eco} (Figure 2c,d) in Kevo (average $VPD_{branch} -$
 330 $VPD_{eco} = 0.30$ kPa) compared to Abisko (average $VPD_{branch} - VPD_{eco} = 0.14$ kPa). Kevo
 331 also received heavier and more frequent precipitation (Figure 2e,f), resulting in higher
 332 total growing season precipitation (167.5 mm) compared to Abisko (126.6 mm).

333 Both T_{leaf} and ET_{eco} tended to be higher in Abisko than in Kevo, on average 50% higher
 334 for T_{leaf} and 62% higher for ET_{eco} . Their seasonal dynamics were similar and followed

1
2
3 335 the course of evaporative demand (Figure 2g-j). However, some differences between
4
5 336 T_{leaf} and ET_{eco} during the early growing season (before DOY 160) were apparent for
6
7 337 Abisko. The diurnal cycles of evaporative fluxes and their drivers varied seasonally in
8
9 338 both sites (Figure S2, S3), as expected due to the changing daylight hours at these
10
11 339 latitudes. Abisko typically presented higher ET_{eco} and T_{leaf} except during the late season,
12
13 340 when T_{leaf} was equal for the two sites.

14 341 3. 2. Modelling environmental controls of evaporative fluxes

15
16 342 ET_{eco} and T_{leaf} increased with PAR and VPD but the relationship with VPD showed
17
18 343 much less scatter (Figure 3). In general, T_{leaf} and ET_{eco} at a given value of PAR or VPD
19
20 344 were higher for Abisko. Models of ET_{eco} and T_{leaf} showed a good predictive ability, with
21
22 345 marginal R^2 values > 0.7 (Table 2,3). Model predictors included a negative interaction
23
24 346 between PAR and VPD but did not include SMD (Table 2,3). The environmental
25
26 347 responses of ET_{eco} did not vary across sites and we only detected site differences for the
27
28 348 intercept and the PAR coefficient in the T_{leaf} model (Table 2,3). In both models, the
29
30 349 interaction between VPD and PAR resulted in complex patterns in the variation of T_{leaf}
31
32 350 and ET_{eco} (Figure 4). For example, for T_{leaf} , steeper relationships with VPD_{branch} were
33
34 351 predicted at low PAR_{branch} in both sites. In Abisko, higher ET_{eco} was predicted under
35
36 352 conditions of high PAR_{eco} and low VPD_{eco} values (Figure 4).

37 353 3. 3. Overstorey and understorey contributions to ecosystem evapotranspiration

38
39 354 Higher spatial variability of LAI in Abisko (Table 1) translated into a much larger
40
41 355 variability in T_{birch} , while T_{birch} was lower and less variable in Kevo (Figure 5). On
42
43 356 average, the daily contribution of mean T_{birch} to ET_{eco} reached peak values of *ca.* 65% in
44
45 357 Abisko and *ca.* 30% in Kevo. However, the highly variable LAI in Abisko (Table 1)
46
47 358 resulted in the upper bound of T_{birch}/ET_{eco} occasionally approaching 100% at this
48
49 359 location (Figure 5c).

50 360 The value of T_{birch}/ET_{eco} increased with VPD_{eco} and PAR_{eco} (both log-transformed;
51
52 361 Table S4, Figure 6a,b). In both cases, model selection retained the interaction between
53
54 362 site and the environmental variable, but it was not significant for either driver (Table
55
56 363 S4). We did not detect any effect of SMD on T_{birch}/ET_{eco} (Figure 6c; Table S4). We did
57
58 364 not find any difference in T_{birch}/ET_{eco} between dry and wet days ($p = 0.27$).

1
2
3 365 The mean growing season contribution of T_{birch} to ET_{eco} was relatively low in Abisko
4 366 (*ca.* 33%) but it was even lower in Kevo (16%, Table 4). Daily evapotranspiration by
5 367 understorey components in Kevo was generally lower compared to T_{birch} (Figure 5d).
6
7 368 For the whole of the growing season, $ET_{upscaled}$ only amounted to *ca.* 40% of ET_{eco} in
8
9 369 Kevo (Table 4).

10
11
12 370 Daily ET_{eco} was higher in Abisko (Figure 5a,b), which also showed higher growing
13 371 season totals compared to Kevo (Table 4). Remarkably, in Abisko ET_{eco} was 27%
14 372 higher than the precipitation in the same period, while in Kevo the ecosystem returned
15 373 to the atmosphere only *ca.* 59% of precipitation (ET_{eco}/P , Table 4). Nevertheless, the
16 374 relative role of mountain birch transpiration in recycling precipitation was much higher
17 375 in Abisko than in Kevo (T_{birch}/P , Table 4).

18
19
20
21
22
23 376

24 377 **4. Discussion**

25 26 378 *4.1. Differences in seasonal and environmental controls on transpiration and* 27 28 379 *evapotranspiration between sites*

29
30
31
32 380 Boreal and arctic regions are undergoing very rapid and pronounced climatic warming,
33 381 which is expected to modify water and energy fluxes across much of the terrestrial
34 382 biosphere of these northern regions. We find that controls of evaporative fluxes by
35 383 mixed birch-tundra communities of Northern Fennoscandia largely consist of controls
36 384 by VPD (which strongly depends on air and canopy temperature) and by PAR. The
37 385 relative importance of these effects depended partly on specific site conditions and the
38 386 scale (branch versus ecosystem) at which they were considered. Predicted increases in
39 387 air temperature can therefore be expected to increase the relative contribution of VPD
40 388 relative to PAR in controlling evaporative fluxes.

41
42
43
44 389 Conversely, we find that the evaporative fluxes are not affected by temporal changes in
45 390 soil moisture, suggesting that water supply is currently not a major limiting factor to
46 391 evapotranspiration. Thus, there were no edaphic drought stress effects in T_{leaf} regulation
47 392 by mountain birch, confirming results observed for other birch species (Gartner,
48 393 Nadezhdina, Englisch, Čermak, & Leitgeb, 2009; Yan et al., 2018). Our results at the
49 394 ecosystem level are consistent with field studies in forest-tundra systems (Beringer et

1
2
3 395 al., 2005) and with a recent data synthesis, where no effect of soil moisture was reported
4
5 396 for evapotranspiration at high latitudes (Kasurinen et al., 2014). Nevertheless,
6
7 397 evaporative fluxes in boreal forests in more continental climates, with higher
8
9 398 evaporative demands, may be influenced by soil moisture (Ohta et al., 2008).

10
11 399 At the seasonal time scale, fluxes were primarily controlled by LAI dynamics at both
12
13 400 sites (cf. Poyatos et al., 2012). Seasonal courses of T_{leaf} and ET_{eco} mirrored each other,
14
15 401 except during the start of the growing season in Abisko, when the discrepancy between
16
17 402 T_{leaf} and ET_{eco} may have been caused by combined errors in the quantification of low
18
19 403 fluxes and leaf area during early leaf development. Alternatively, this temporal
20
21 404 mismatch between T_{leaf} and ET_{eco} may have been driven by substantial evaporation from
22
23 405 moist soils after snowmelt and/or spatial variability in the phenology of greening up
24
25 406 between the measured branches and the rest of the forest.

26
27 407 Both T_{leaf} and ET_{eco} were higher in Abisko than in Kevo because of the generally higher
28
29 408 evaporative demand in Abisko (Figure 2). Environmental controls on T_{leaf} were very
30
31 409 similar across sites. The only significant difference in the response of T_{leaf} to PAR may
32
33 410 be due to differences in stand structure at the plot level (Table 1). The responses of
34
35 411 evaporative fluxes to PAR and VPD differed between the two sites more clearly for T_{leaf}
36
37 412 than for ET_{eco} , suggesting a higher sensitivity to VPD of the birch canopy compared to
38
39 413 other ecosystem components (see also section 4.2). The negative interaction between
40
41 414 VPD and PAR produced complex response surfaces of evaporative fluxes to
42
43 415 environmental conditions. Model responses during conditions of high evaporative
44
45 416 demand were reasonable, apart from those by ET_{eco} at Abisko, where the model showed
46
47 417 a decrease of ET_{eco} with VPD at high PAR. The more extreme responses were found for
48
49 418 unrealistic combinations of environmental conditions, which are not usually found in
50
51 419 the field. (i.e. high VPD and low PAR), and when the model's predictions of the
52
53 420 interaction effects are less reliable.

54
55 421

56 57 422 *4.2. Contribution of mountain birch transpiration to ecosystem evapotranspiration* 58 59 423 *across sites and environmental conditions*

60
61 424 The mean daily contribution of birch transpiration to ecosystem evapotranspiration (i.e.
62
63 425 T_{birch}/ET_{eco}) was much higher in Abisko than in Kevo. In Abisko, the higher variability

1
2
3 426 in LAI at the landscape level propagates to a larger range of T_{birch}/ET_{eco} values
4
5 427 compared to Kevo. When explaining seasonal variability in T_{birch}/ET_{eco} , we found that
6
7 428 T_{birch}/ET_{eco} strongly depended on VPD and PAR, with T_{birch}/ET_{eco} saturating at high
8
9 429 VPD, but this environmental control on T_{birch}/ET_{eco} was stronger in Abisko. Therefore,
10
11 430 our results show an increased relative role of mountain birch in controlling ecosystem
12
13 431 evapotranspiration as evaporative demand increases, especially in denser forests, in
14
15 432 contrast with studies on waterlogged peatlands where understorey contribution increases
16
17 433 with VPD (Ikawa et al., 2015). In our sites, mountain birch roots possibly access soil
18
19 434 moisture at greater depths (Hunziker, Sigurdsson, Halldorsson, Schwanghart, & Kuhn,
20
21 435 2014), supplying water to meet the increasing evaporative demand and causing the
22
23 436 increase in T_{birch}/ET_{eco} .

24
25 437 At the growing season level, birch transpiration contributed *ca.* 33% of total ecosystem
26
27 438 evapotranspiration in Abisko but the contribution was only *ca.* 16% in Kevo (Table 4).
28
29 439 These differences were attributable not only to a higher birch LAI in Abisko (Table 1),
30
31 440 but also to the higher T_{leaf} values at this site (Figure 2). Lower T_{birch}/ET_{eco} values in
32
33 441 Kevo could also result from a disproportionately higher contribution from the
34
35 442 understorey in a sparser woodland (i.e. higher below-canopy incident radiation
36
37 443 compared to Abisko). The values of T_{birch}/ET_{eco} at the two sites are consistent with
38
39 444 the generally low contribution of overstorey to total evapotranspiration in subarctic and
40
41 445 northern boreal forests (Iida et al., 2009; Ikawa et al., 2015; Kelliher et al., 1997;
42
43 446 Lafleur, 1992; Warren et al., 2019). However, in Kevo, our estimates of upscaled
44
45 447 evapotranspiration from individual ecosystem components (i.e. mountain birch,
46
47 448 understorey shrubs and lichen heath) yielded growing season values, which were still
48
49 449 far from total ecosystem evapotranspiration measured by eddy covariance (Table 4, cf.
50
51 450 section 4.3). In the following section, we discuss potential methodological artefacts and
52
53 451 unmeasured processes that could explain this discrepancy.

54 452 *4.3. Methodological considerations*

55
56 453 This study jointly analyses a multi-scale dataset of evaporative fluxes from subarctic
57
58 454 forest communities. Comparing evaporative fluxes across scales is hindered by the
59
60 455 numerous potential errors associated with measurement techniques and upscaling
61
62 456 procedures. Transpiration measurements from closed chambers could have been

1
2
3 457 affected by radiation-driven overheating (Poyatos et al., 2012), by raising VPD_{branch}
4 458 above VPD_{eco} and causing an overestimation of T_{leaf} . However, the relatively low values
5 459 of T_{birch} and $ET_{upscaled}$, both based on closed chamber measurements, do not suggest that
6
7 460 the conclusions of this study could have been affected by this artefact.
8
9

10 461 The upscaling procedure also has a number of potential limitations that warrant
11 462 consideration. Due to the sparseness of the forest in Kevo (i.e. little shading effects on
12 463 understorey vegetation), we assumed that the magnitude and regulation of understorey
13 464 evapotranspiration was similar to that shown by patches with similar composition in the
14 465 forest-tundra transition (Poyatos et al., 2014). However, LAI of the patches measured
15 466 with automated chambers in the forest-mire transition (see section 2.5) was *ca.* 50% of
16 467 the LAI actually measured in survey plots located within the forest (Table 1). Rescaling
17 468 the understorey fluxes according to this understorey LAI, evapotranspiration from
18 469 understorey components at the ecosystem level would be amount to 23.6 mm, an
19 470 evaporative flux 55% larger than T_{birch} . Scaling-up evapotranspiration estimated from
20 471 canopy and understorey components, accounting for their land cover fractions and
21 472 applying the LAI correction outlined above to understorey measurements would
22 473 increase growing season $ET_{upscaled}$ values to 44.4 mm, or *ca.* 45% of ET_{eco} .
23
24
25
26
27
28
29
30
31
32

33 474 4.4. Differences in growing season water balance across sites

34 475 Even accounting for this likely underestimation of ET_{shrub} and ET_{lichen} , there is still a
35 476 fraction of ET_{eco} that cannot be explained by upscaled gas exchange measurements from
36 477 individual ecosystem components. Taking into account that T_{birch} obtained from branch-
37 478 bag measurements excludes evaporation of intercepted water, we showed that
38 479 T_{birch}/ET_{eco} does not vary between dry and wet days. This may suggest that evaporation
39 480 of intercepted water may not be captured by eddy covariance measurements, otherwise
40 481 T_{birch}/ET_{eco} would have been lower on wet days than dry days. Potentially high
41 482 evaporation rates after precipitation may be partially missed from ET_{eco} and $ET_{upscaled}$,
42 483 because data from open-path gas analysers are removed when the sensor windows are
43 484 wet and subsequent gap-filling would not account for the missed evaporation of
44 485 intercepted water (Oishi, Oren, & Stoy, 2008). Combined interception by overstorey
45 486 canopies and mosses in northern boreal forests may amount up to 40% of bulk
46
47
48
49
50
51
52
53
54
55
56
57
58
59
60

1
2
3 487 precipitation (Price, Dunham, Carleton, & Band, 1997), and we are not currently
4
5 488 accounting for this substantial contribution.
6

7 489 We found stark differences between sites in the percentage of precipitation returned to
8
9 490 the atmosphere as evapotranspiration; the mountain birch woodland in Abisko
10
11 491 evaporated more water than it received during the growing season, as observed in other
12
13 492 deciduous boreal forests (Blanken et al., 2001; Kelliher et al., 1997). In contrast, Kevo
14
15 493 showed a substantial water surplus (Table 4). Our measurements did not include the
16
17 494 snowmelt period, but these sites can reach snowpack depths of > 1 m (data for Kevo,
18
19 495 2009) and tree water uptake during this period, especially from deciduous species, can
20
21 496 progressively deplete soil water sources (Young-Robertson et al., 2016). This decline in
22
23 497 soil water content after snowmelt is very clear in the seasonal course of SMD measured
24
25 498 in Abisko in 2008 and 2009 (outside our measurement period in Abisko, Fig S5).
26
27 499 Therefore, these differences in the role of the mountain birch canopy between Abisko
28
29 500 and Kevo, mediated by their different stand structure, can illustrate the potential
30
31 501 changes in the hydrological regime that can result from the expansion and densification
32
33 502 of subarctic deciduous woodlands.

34 503 *4.5. Concluding remarks*

35 504 We have shown that the dominant mountain birch canopy plays only a partial role in
36
37 505 driving ecosystem evapotranspiration in both subarctic sites, and this may be a general
38
39 506 feature of low-LAI subarctic and northern boreal forests (Saugier, Granier, Pontailier,
40
41 507 Dufrene, & Baldocchi, 1997). Our results also show that both increased woodland cover
42
43 508 and increased woodland density under climate change conditions (Rundqvist et al.,
44
45 509 2011) will result in larger controls of the water fluxes by the canopies of deciduous trees
46
47 510 as opposed to the understorey vegetation. However, our upscaling exercise also shows
48
49 511 that adequately accounting for understorey components (and transpiration vs
50
51 512 evaporation processes; Stoy et al., 2019) may be necessary to constrain future
52
53 513 hydrological changes in these areas. The highly variable and patchy nature of subarctic
54
55 514 vegetation may require flux upscaling approaches considering spatial variation not only
56
57 515 of land cover (Hartley et al., 2015), but also of LAI (Stoy et al., 2013).

58 516 In the longer term, shifts towards deciduous-dominated communities in subarctic
59
60 517 regions and an increased land cover by forest as opposed to tundra are expected to

1
2
3 518 induce large hydro-climatic effects. These effects are expected to be mediated by higher
4
5 519 transpiration rates, inducing complex land-climate feedbacks (Bonfils et al., 2012;
6
7 520 Swann et al., 2010), which need to be considered together with carbon- and energy-
8
9 521 related feedbacks (Wit et al., 2014). Overall, combining several flux datasets and land
10
11 522 cover information we provide, for the poorly studied subarctic deciduous woodlands,
12
13 523 highly valuable results that will help to calibrate and validate evapotranspiration
14
15 524 processes in ecosystem models.

16 525 **Acknowledgements**

17
18 526 AM. Sabater is supported by European Social Fund and Generalitat Valenciana (GVA)
19
20 527 under a PhD contract (ACIF – 2017/9830). This study was funded by the following
21
22 528 grants: ABACUS NE/D005795/1 (NERC, UK), SAPFLUXNET CGL2014-JIN-55583
23
24 529 (MINECO, Spain), VERSUS CGL2015-67466-R (MINECO/FEDER), SGR-2017-1001
25
26 530 (AGAUR, Generalitat de Catalunya) and IMAGINA PROMETEU/2019/110
27
28 531 (Conselleria de Cultura, GVA). We are grateful for the support by the staff at the Kevo
29
30 532 Subarctic Research Institute and at the Abisko Research Station. We would also like to
31
32 533 acknowledge the help in the field by T. August, A. Robertson, K. Leslie, D. Sayer and
33
34 534 J.R.M. Allen.

35 535

36 536 **References**

- 37
38
39 Aubinet, M., Vesala, T., & Papale, D. (2012). *Eddy Covariance: A Practical Guide to*
40 *Measurement and Data Analysis*. Springer Science & Business Media.
41
42 Beringer, J., Chapin, F. S., Thompson, C. C., & McGuire, A. D. (2005). Surface energy
43 exchanges along a tundra-forest transition and feedbacks to climate. *Agricultural*
44 *and Forest Meteorology*, *131*(3–4), 143–161.
45
46 Blanken, P. D., Black, T. A., Neumann, H. H., den Hartog, G., Yang, P. C., Nesic, Z., &
47 Lee, X. (2001). The seasonal water and energy exchange above and within a
48 boreal aspen forest. *Journal of Hydrology*, *245*(1–4), 118–136.
49 [https://doi.org/10.1016/S0022-1694\(01\)00343-2](https://doi.org/10.1016/S0022-1694(01)00343-2)
50
51 Bonan, G. B. (2008). Forests and Climate Change: Forcings, Feedbacks, and the
52 Climate Benefits of Forests. *Science*, *320*, 1444–1449.
53 <https://doi.org/10.1126/science.1155121>
54
55 Bonfils, C. J. W., Phillips, T. J., Lawrence, D. M., Cameron-Smith, P., Riley, W. J., &
56 Subin, Z. M. (2012). On the influence of shrub height and expansion on northern
57 high latitude climate. *Environmental Research Letters*, *7*(1), 015503.
58 <https://doi.org/10.1088/1748-9326/7/1/015503>

- 1
2
3 Brümmer, C., Black, T. A., Jassal, R. S., Grant, N. J., Spittlehouse, D. L., Chen, B., ...
4 Wofsy, S. C. (2011). How climate and vegetation type influence
5 evapotranspiration and water use efficiency in Canadian forest, peatland and
6 grassland ecosystems. *Agricultural and Forest Meteorology*.
7 <https://doi.org/10.1016/j.agrformet.2011.04.008>
8
9 Callaghan, T. V., Björn, L. O., Chapin Iii, F., Chernov, Y., Christensen, T. R., Huntley,
10 B., ... Shaver, G. R. (2005). Arctic tundra and polar desert ecosystems. In *Arctic*
11 *climate impact assessment* (Vol. 1, pp. 243–352).
12
13 Callaghan, T. V., Jonasson, C., Thierfelder, T., Yang, Z., Hedenås, H., Johansson, M.,
14 ... Sloan, V. L. (2013). Ecosystem change and stability over multiple decades in
15 the Swedish subarctic: Complex processes and multiple drivers. *Philosophical*
16 *Transactions of the Royal Society B: Biological Sciences*, 368(1624), 20120488.
17 <https://doi.org/10.1098/rstb.2012.0488>
18
19 Chapin, F. S., Mcguire, A. D., Randerson, J., Pielke, R., Baldocchi, D., Hobbie, S. E.,
20 ... Running, S. W. (2000). Arctic and boreal ecosystems of western North
21 America as components of the climate system. *Global Change Biology*, 6(S1),
22 211–223. <https://doi.org/10.1046/j.1365-2486.2000.06022.x>
23
24 Cohen, L. R., Raz-Yaseef, N., Curtis, J. B., Young, J. M., Rahn, T. A., Wilson, C. J., ...
25 Newman, B. D. (2015). Measuring diurnal cycles of evapotranspiration in the
26 Arctic with an automated chamber system. *Ecohydrology*, 8(4), 652–659.
27 <https://doi.org/10.1002/eco.1532>
28
29 Dahlberg, U., Berge, T. W., Petersson, H., & Vencatasawmy, C. P. (2004). Modelling
30 biomass and leaf area index in a sub-arctic Scandinavian mountain area.
31 *Scandinavian Journal of Forest Research*, 19, 60–71.
32 <https://doi.org/10.1080/02827580310019266>
33
34 Fletcher, B. J., Gornall, J. L., Poyatos, R., Press, M. C., Stoy, P. C., Huntley, B., ...
35 Phoenix, G. K. (2012). Photosynthesis and productivity in heterogeneous arctic
36 tundra: Consequences for ecosystem function of mixing vegetation types at
37 stand edges. *Journal of Ecology*, 100(2), 441–451.
38 <https://doi.org/10.1111/j.1365-2745.2011.01913.x>
39
40 Gartner, K., Nadezhdina, N., Englisch, M., Čermak, J., & Leitgeb, E. (2009). Sap flow
41 of birch and Norway spruce during the European heat and drought in summer
42 2003. *Forest Ecology and Management*, 258(5), 590–599.
43 <https://doi.org/10.1016/j.foreco.2009.04.028>
44
45 Gash, J. H. C., & Dolman, A. J. (2003). Sonic anemometer (co)sine response and flux
46 measurement: I. The potential for (co)sine error to affect sonic anemometer-
47 based flux measurements. *Agricultural and Forest Meteorology*, 119(3), 195–
48 207. [https://doi.org/10.1016/S0168-1923\(03\)00137-0](https://doi.org/10.1016/S0168-1923(03)00137-0)
49
50 Granier, A., & Loustau, D. (1994). Measuring and modelling the transpiration of a
51 maritime pine canopy from sap-flow data. *Agricultural and Forest Meteorology*,
52 71, 61–81.
53
54 Grelle, A., Lundberg, A., Lindroth, A., Morén, A.-S., & Cienciala, E. (1997).
55 Evaporation components of a boreal forest: Variations during the growing
56 season. *Journal of Hydrology*, 197(1), 70–87. [https://doi.org/10.1016/S0022-1694\(96\)03267-2](https://doi.org/10.1016/S0022-1694(96)03267-2)
57
58 Haapanala, S., Ekberg, A., Hakola, H., Tarvainen, V., Rinne, J., Hellén, H., & Arneht,
59 A. (2009). Mountain birch–potentially large source of sesquiterpenes into high
60 latitude atmosphere. *Biogeosciences*, 6, 2709–2718.

- 1
2
3 Hartley, I. P., Hopkins, D. W., Sommerkorn, M., & Wookey, P. A. (2010). The
4 response of organic matter mineralisation to nutrient and substrate additions in
5 sub-arctic soils. *Soil Biology and Biochemistry*, *42*(1), 92–100.
- 6 Hartley, Iain. P., Hill, Timothy. C., Wade, Thomas. J., Clement, Robert. J., Moncrieff,
7 John. B., Prieto-Blanco, Ana., ... Baxter, Robert. (2015). Quantifying
8 landscape-level methane fluxes in subarctic Finland using a multiscale approach.
9 *Global Change Biology*, *21*(10), 3712–3725. <https://doi.org/10.1111/gcb.12975>
- 10 Hofgaard, A., Tømmervik, H., Rees, G., & Hanssen, F. (2013). Latitudinal forest
11 advance in northernmost Norway since the early 20th century. *Journal of*
12 *Biogeography*, *40*(5), 938–949. <https://doi.org/10.1111/jbi.12053>
- 13 Hunziker, M., Sigurdsson, B. D., Halldorsson, G., Schwanghart, W., & Kuhn, N.
14 (2014). Biomass allometries and coarse root biomass distribution of mountain
15 birch in southern Iceland. *Icelandic Agricultural Sciences*, *27*, 111–125.
- 16 Iida, S., Ohta, T., Matsumoto, K., Nakai, T., Kuwada, T., Kononov, A. V., ... Yabuki,
17 H. (2009). Evapotranspiration from understory vegetation in an eastern Siberian
18 boreal larch forest. *Agricultural and Forest Meteorology*, *149*(6), 1129–1139.
19 <https://doi.org/10.1016/j.agrformet.2009.02.003>
- 20 Ikawa, H., Nakai, T., Busey, R. C., Kim, Y., Kobayashi, H., Nagai, S., ... Hinzman, L.
21 (2015). Understory CO₂, sensible heat, and latent heat fluxes in a black spruce
22 forest in interior Alaska. *Agricultural and Forest Meteorology*, *214–215*, 80–90.
23 <https://doi.org/10.1016/j.agrformet.2015.08.247>
- 24 IPCC. (2013). *Climate Change 2013: The Physical Science Basis. Contribution of*
25 *Working Group I to the Fifth Assessment Report of the Intergovernmental Panel*
26 *on Climate Change*. <https://doi.org/10.1017/CBO9781107415324>
- 27 Kasurinen, V., Alfredsen, K., Kolari, P., Mammarella, I., Alekseychik, P., Rinne, J., ...
28 Berninger, F. (2014). Latent heat exchange in the boreal and arctic biomes.
29 *Global Change Biology*, *20*(11), 3439–3456. <https://doi.org/10.1111/gcb.12640>
- 30 Kattsov, V. M., Källén, E., Cattle, H. P., Christensen, J., Drange, H., Hanssen-Bauer, I.,
31 ... others. (2005). *Future climate change: Modeling and scenarios for the*
32 *Arctic*.
- 33 Kelliher, F. M., Hollinger, D. Y., Schulze, E.-D., Vygodskaya, N. N., Byers, J. N.,
34 Hunt, J. E., ... Bauer, G. (1997). Evaporation from an eastern Siberian larch
35 forest. *Agricultural and Forest Meteorology*, *85*(3), 135–147.
36 [https://doi.org/10.1016/S0168-1923\(96\)02424-0](https://doi.org/10.1016/S0168-1923(96)02424-0)
- 37 Knauer, J., Werner, C., & Zaehle, S. (2015). Evaluating stomatal models and their
38 atmospheric drought response in a land surface scheme: A multibiome analysis.
39 *Journal of Geophysical Research: Biogeosciences*, *120*(10), 2015JG003114.
40 <https://doi.org/10.1002/2015JG003114>
- 41 Krankina, O. N., Pflugmacher, D., Hayes, D. J., McGuire, A. D., Hansen, M. C., Häme,
42 T., ... Nelson, P. (2010). Vegetation cover in the eurasian arctic: Distribution,
43 monitoring, and role in carbon cycling. In *Eurasian arctic land cover and land*
44 *use in a changing climate* (pp. 79–108). Springer.
- 45 Lafleur, P. M. (1992). Energy balance and evapotranspiration from a subarctic forest.
46 *Agricultural and Forest Meteorology*, *58*(3–4), 163–175.
47 [https://doi.org/10.1016/0168-1923\(92\)90059-D](https://doi.org/10.1016/0168-1923(92)90059-D)
- 48 McFadden, J. P., Eugster, W., & Chapin III, F. S. (2003). A regional study of the
49 controls on water vapor and CO₂ exchange in arctic tundra. *Ecology*, *84*(10),
50 2762–2776.
- 51
52
53
54
55
56
57
58
59
60

- 1
2
3 Mekonnen, Z. A., Riley, W. J., Randerson, J. T., Grant, R. F., & Rogers, B. M. (2019).
4 Expansion of high-latitude deciduous forests driven by interactions between
5 climate warming and fire. *Nature Plants*, 1–7. [https://doi.org/10.1038/s41477-](https://doi.org/10.1038/s41477-019-0495-8)
6 [019-0495-8](https://doi.org/10.1038/s41477-019-0495-8)
7
8 Myers-Smith, I. H., Forbes, B. C., Wilmsking, M., Hallinger, M., Lantz, T., Blok, D., ...
9 Hik, D. S. (2011). Shrub expansion in tundra ecosystems: Dynamics, impacts
10 and research priorities. *Environmental Research Letters*, 6(4), 045509.
11 <https://doi.org/10.1088/1748-9326/6/4/045509>
12
13 Nakagawa, S., & Schielzeth, H. (2013). A general and simple method for obtaining R²
14 from generalized linear mixed-effects models. *Methods in Ecology and*
15 *Evolution*, 4(2), 133–142. <https://doi.org/10.1111/j.2041-210x.2012.00261.x>
16
17 Nyström, M., Holmgren, J., & Olsson, H. (2012). Prediction of tree biomass in the
18 forest–tundra ecotone using airborne laser scanning. *Remote Sensing of*
19 *Environment*, 123, 271–279. <https://doi.org/10.1016/j.rse.2012.03.008>
20
21 Ohta, T., Maximov, T. C., Dolman, A. J., Nakai, T., van der Molen, M. K., Kononov,
22 A. V., ... Yabuki, H. (2008). Interannual variation of water balance and summer
23 evapotranspiration in an eastern Siberian larch forest over a 7-year period
24 (1998–2006). *Agricultural and Forest Meteorology*, 148(12), 1941–1953.
25 <https://doi.org/10.1016/j.agrformet.2008.04.012>
26
27 Oishi, A. C., Oren, R., & Stoy, P. C. (2008). Estimating components of forest
28 evapotranspiration: A footprint approach for scaling sap flux measurements.
29 *Agricultural and Forest Meteorology*, 148(11), 1719–1732.
30
31 Pinheiro, J., Bates, D., DebRoy, S., Sarkar, D., & R Core Team. (2018). *nlme: Linear*
32 *and Nonlinear Mixed Effects Models*. Retrieved from [https://CRAN.R-](https://CRAN.R-project.org/package=nlme)
33 [project.org/package=nlme](https://CRAN.R-project.org/package=nlme)
34
35 Poyatos, R., Gornall, J., Mencuccini, M., Huntley, B., & Baxter, R. (2012). Seasonal
36 controls on net branch CO₂ assimilation in sub-Arctic Mountain Birch (*Betula*
37 *pubescens* ssp. *Czerepanovii* (Orlova) Hamet-Ahti). *Agricultural and Forest*
38 *Meteorology*, 158–159, 90–100. <https://doi.org/10.1016/j.agrformet.2012.02.009>
39
40 Poyatos, R., Heinemeyer, A., Ineson, P., Evans, J. G., Ward, H. C., Huntley, B., &
41 Baxter, R. (2014). Environmental and Vegetation Drivers of Seasonal CO₂
42 Fluxes in a Sub-arctic Forest–Mire Ecotone. *Ecosystems*, 17(3), 377–393.
43 <https://doi.org/10.1007/s10021-013-9728-2>
44
45 Price, A. G., Dunham, K., Carleton, T., & Band, L. (1997). Variability of water fluxes
46 through the black spruce (*Picea mariana*) canopy and feather moss (*Pleurozium*
47 *schreberi*) carpet in the boreal forest of Northern Manitoba. *Journal of*
48 *Hydrology*, 196(1), 310–323. [https://doi.org/10.1016/S0022-1694\(96\)03233-7](https://doi.org/10.1016/S0022-1694(96)03233-7)
49
50 Rayment, M. B., & Jarvis, P. G. (1999). Seasonal gas exchange of black spruce using an
51 automatic branch bag system. *Canadian Journal of Forest Research*, 29, 1528–
52 1538.
53
54 Rundqvist, S., Hedenås, H., Sandström, A., Emanuelsson, U., Eriksson, H., Jonasson,
55 C., & Callaghan, T. V. (2011). Tree and Shrub Expansion Over the Past 34
56 Years at the Tree-Line Near Abisko, Sweden. *AMBIO: A Journal of the Human*
57 *Environment*, 40(6), 683–692. <https://doi.org/10.1007/s13280-011-0174-0>
58
59 Saugier, B., Granier, A., Pontailier, J. Y., Dufrene, E., & Baldocchi, D. D. (1997).
60 Transpiration of a boreal pine forest measured by branch bag, sap flow and
micrometeorological methods. *Tree Physiology*, 17, 511–519.

- Schlesinger, W. H., & Jasechko, S. (2014). Transpiration in the global water cycle. *Agricultural and Forest Meteorology*, 189–190, 115–117. <https://doi.org/10.1016/j.agrformet.2014.01.011>
- Schotanus, P., Nieuwstadt, F. T. M., & De Bruin, H. A. R. (1983). Temperature measurement with a sonic anemometer and its application to heat and moisture fluxes. *Boundary-Layer Meteorology*, 26(1), 81–93. <https://doi.org/10.1007/BF00164332>
- Stoy, P. C., Williams, M., Evans, J. G., Prieto-Blanco, A., Disney, M., Hill, T. C., ... Street, L. E. (2013). Upscaling tundra CO₂ exchange from chamber to eddy covariance tower. *Arctic, Antarctic, and Alpine Research*, 45(2), 275–284.
- Stoy, Paul C., El-Madany, T. S., Fisher, J. B., Gentine, P., Gerken, T., Good, S. P., ... Wolf, S. (2019). Reviews and syntheses: Turning the challenges of partitioning ecosystem evaporation and transpiration into opportunities. *Biogeosciences*, 16(19), 3747–3775. <https://doi.org/10.5194/bg-16-3747-2019>
- Stoy, Paul C., Mauder, M., Foken, T., Marcolla, B., Boegh, E., Ibrom, A., ... Varlagin, A. (2013). A data-driven analysis of energy balance closure across FLUXNET research sites: The role of landscape scale heterogeneity. *Agricultural and Forest Meteorology*, 171–172, 137–152. <https://doi.org/10.1016/j.agrformet.2012.11.004>
- Swann, A. L., Fung, I. Y., Levis, S., Bonan, G. B., & Doney, S. C. (2010). Changes in Arctic vegetation amplify high-latitude warming through the greenhouse effect. *Proceedings of the National Academy of Sciences*, 107(4), 1295–1300. <https://doi.org/10.1073/pnas.0913846107>
- Tømmervik, H., Johansen, B., Tombre, I., Thannheiser, D., Høgda, K. A., Gaare, E., & Wielgolaski, F. E. (2004). Vegetation Changes in the Nordic Mountain Birch Forest: The Influence of Grazing and Climate Change. *Arctic, Antarctic, and Alpine Research*, 36(3), 323–332.
- Wang, J. A., Sulla-Menashe, D., Woodcock, C. E., Sonnentag, O., Keeling, R. F., & Friedl, M. A. (2019). Extensive land cover change across Arctic–Boreal Northwestern North America from disturbance and climate forcing. *Global Change Biology*, 0(0). <https://doi.org/10.1111/gcb.14804>
- Warren, R. K., Pappas, C., Helbig, M., Chasmer, L. E., Berg, A. A., Baltzer, J. L., ... Sonnentag, O. (2019). Minor contribution of overstorey transpiration to landscape evapotranspiration in boreal permafrost peatlands. *Ecohydrology*, 11(5), e1975. <https://doi.org/10.1002/eco.1975>
- Webb, E. K., Pearman, G. I., & Leuning, R. (1980). Correction of flux measurements for density effects due to heat and water vapour transfer. *Quarterly Journal of the Royal Meteorological Society*, 106(447), 85–100. <https://doi.org/10.1002/qj.49710644707>
- Welp, L. R., Randerson, J. T., & Liu, H. P. (2007). The sensitivity of carbon fluxes to spring warming and summer drought depends on plant functional type in boreal forest ecosystems. *Agricultural & Forest Meteorology*, 147(3–4), 172–185.
- Wingate, L., Seibt, U., Moncrieff, J. B., Jarvis, P. G., & Lloyd, J. (2007). Variations in ¹³C discrimination during CO₂ exchange by *Picea sitchensis* branches in the field. *Plant, Cell & Environment*, 30(5), 600–616. <https://doi.org/10.1111/j.1365-3040.2007.01647.x>
- Wit, H. A. de, Bryn, A., Hofgaard, A., Karstensen, J., Kvælevåg, M. M., & Peters, G. P. (2014). Climate warming feedback from mountain birch forest expansion:

- 1
2
3 Reduced albedo dominates carbon uptake. *Global Change Biology*, 20(7), 2344–
4 2355. <https://doi.org/10.1111/gcb.12483>
5 Yan, C., Wang, B., Zhang, Y., Zhang, X., Takeuchi, S., & Qiu, G. (2018). Responses of
6 Sap Flow of Deciduous and Conifer Trees to Soil Drying in a Subalpine Forest.
7 *Forests*, 9(1), 32. <https://doi.org/10.3390/f9010032>
8 Young-Robertson, J. M., Bolton, W. R., Bhatt, U. S., Cristóbal, J., & Thoman, R.
9 (2016). Deciduous trees are a large and overlooked sink for snowmelt water in
10 the boreal forest. *Scientific Reports*, 6, srep29504.
11 <https://doi.org/10.1038/srep29504>
12 Zhang, W., Miller, P. A., Smith, B., Wania, R., Koenigk, T., & Döscher, R. (2013).
13 Tundra shrubification and tree-line advance amplify arctic climate warming:
14 Results from an individual-based dynamic vegetation model. *Environmental*
15 *Research Letters*, 8(3), 034023. <https://doi.org/10.1088/1748-9326/8/3/034023>
16 Zuur, A. F., Ieno, E. N., & Elphick, C. S. (2010). A protocol for data exploration to
17 avoid common statistical problems. *Methods in Ecology and Evolution*, 1(1), 3–
18 14. <https://doi.org/10.1111/j.2041-210X.2009.00001.x>
19
20
21
22
23
24
25
26
27
28
29
30
31
32
33
34
35
36
37
38
39
40
41
42
43
44
45
46
47
48
49
50
51
52
53
54
55
56
57
58
59
60

537 **Tables**

538 **Table 1.** Stand characteristics of mountain birch forests in Abisko and Kevo. Values
 539 labelled as 'Site' represent the site mean (\pm SE) of all inventory plots in Abisko (N=6)
 540 and Kevo (N=8). Values labelled as 'BB' are the values of the plots in the vicinity of
 541 the branch bags measuring sites. Tree density refers to polycormic individuals, with
 542 multiple stems per tree.

	Tree density (trees ha ⁻¹)	Stems per tree	Basal area (m ² ha ⁻¹)	DBH (mm)	Height (m)	Overstorey LAI _{max} (m ² m ⁻²)	Understorey LAI _{max} (m ² m ⁻²)
Abisko							
Site	1260 \pm 80	3.7 \pm 0.2	6.5 \pm 0.2	36.9 \pm 1.0	3.9 \pm 0.2	1.2 \pm 0.3	1.0 \pm 0.2
BB	1146	4.4	6.7	35.7	-	1.8	-
Kevo							
Site	876 \pm 85	3.3 \pm 0.2	3.8 \pm 0.4	37.2 \pm 2.0	3.8 \pm 0.0	0.7 \pm 0.1	1.5 \pm 0.1
BB	833	3.8	3.0	30.6	3.8	0.6	-

543

1
2
3
4 544 **Table 2.** Summary statistics of the linear mixed model of log-transformed T_{leaf} as a
5 545 function of environmental variables (VPD_{branch} , PAR_{branch} and SMD) for Abisko and
6 546 Kevo. Asterisks denote significant differences from zero ($*p<0.05$, $**p<0.01$,
7 547 $***p<0.001$). Statistical differences in model coefficients ($p < 0.05$) between Abisko and
8 548 Kevo were marked in bold. SD: Standard deviation. Interactions between variables are
9 549 denoted by colon (:) and variables not included after model selection are denoted by
10 550 'n.i'.

	Abisko	Kevo
Fixed effects		
Intercept	$-2.98 \pm 0.09^*$	$-4.00 \pm 0.07^{***}$
$\log(VPD_{branch})$	$1.26 \pm 0.01^{***}$	$1.27 \pm 0.01^{***}$
PAR_{branch}	$4.1 \cdot 10^{-4} \pm 0.4 \cdot 10^{-4}^{***}$	$7.5 \cdot 10^{-4} \pm 0.4 \cdot 10^{-4}^{***}$
$\log(VPD_{branch}): PAR_{branch}$	$-8.4 \cdot 10^{-4} \pm 0.5 \cdot 10^{-4}^{***}$	$-9.4 \cdot 10^{-4} \pm 0.4 \cdot 10^{-4}^{***}$
SMD	n.i.	n.i.
Random effects (branch)		
SD (Intercept)	0.26	0.20
Residual error	0.40	0.48
Correlation structure (ϕ)	$4.40 \cdot 10^{-8}$	$7.23 \cdot 10^{-7}$
R ² marginal (R ² conditional)	0.78 (0.84)	0.77 (0.80)

551

552 **Table 3.** Summary statistics of the generalised least squares model of ET_{eco} as a
 553 function of environmental variables (VPD_{eco} , PAR_{eco} and SMD) for Abisko and Kevo.
 554 Asterisks denote significant differences from zero ($*p < 0.05$, $**p < 0.01$, $***p < 0.001$). No
 555 significant differences ($p < 0.05$) were found between model coefficients between
 556 Abisko and Kevo. Interactions between variables are denoted by colon (:) and
 557 variables not included after model selection are denoted by 'n.i'.

	Abisko	Kevo
Intercept	$-4.93 \pm 0.38^{***}$	$-4.84 \pm 0.40^{***}$
log(VPD)	$2.58 \pm 0.30^{***}$	$2.13 \pm 0.27^{***}$
log(PAR_{eco})	$0.47 \pm 0.06^{***}$	$0.47 \pm 0.06^{***}$
log(VPD_{eco}):log(PAR_{eco})	$-0.39 \pm 0.05^{***}$	$-0.26 \pm 0.05^{***}$
SMD	n.i.	n.i.
Correlation structure (φ)	$8.23 \cdot 10^{-3}$	$1.84 \cdot 10^{-2}$
R ² marginal	0.71	0.69

558

559

1
2
3 **Table 4.** Growing season values of precipitation (P), birch transpiration (T_{birch}) and
4
5 ecosystem evapotranspiration (ET_{eco}) in Abisko and Kevo. Percentage of evaporative
6
7 fluxes as a fraction of ET_{eco} and P are also shown for growing season values. Values
8
9 with an uncertainty measure represent means \pm standard error.

10
11
12

	Abisko	Kevo
T_{birch} (mm)	52.5 \pm 13.0	15.2 \pm 1.5
ET_{eco} (mm)	160.5	98.5
$ET_{upscaled}$ (mm)	-	39.4 \pm 1.5
T_{birch} / ET_{eco} (%)	32.7 \pm 8.1	15.5 \pm 1.5
T_{birch} / P (%)	41.4 \pm 10.2	9.1 \pm 0.9
ET_{eco} / P (%)	126.6	58.8
$ET_{upscaled} / ET_{eco}$ (%)	-	40.0 \pm 1.5

13
14
15
16
17
18
19
20
21
22
23
24
25
26
27
28
29
30
31
32
33
34
35
36
37
38
39
40
41
42
43
44
45
46
47
48
49
50
51
52
53
54
55
56
57
58
59
60

1
2
3 567 **Figure captions**
4

5 568 **Figure 1.** Study sites at Abisko (a) and Kevo (b), showing the locations of the branch
6 569 bags systems, the eddy flux towers and the understory automated chambers at Kevo.
7 570 Panel (a) shows the aerial photography obtained in Abisko and (b) shows the land
8 571 classification at Kevo obtained from aerial photography (cf. Hartley et al., 2015). *Birch*
9 572 : mountain birch woodland; *Understorey*: low- and dwarf-shrubs; *Lichen*: lichen heath;
10 573 *Mire*: organic hummocks and interhummocks with shrubs and *Spahgnum*; *Water*: open
11 574 water; *Lawns*: graminoid lawns; *Board*: boardwalks; *Other*: other land cover.

12 575 **Figure 2.** Seasonal course of environmental variables and evaporative fluxes (daily
13 576 means) in Abisko and Kevo. Environmental variables include photosynthetically active
14 577 radiation (a-b, PAR), vapour pressure deficit (c-d, VPD) and rainfall (e, f).
15 578 Environmental variables were measured at the ecosystem (black lines) and at the branch
16 579 level (red lines). Mountain birch transpiration per unit leaf area (g-h, T_{leaf}) and
17 580 ecosystem evapotranspiration (i-j, ET_{eco}) are also shown. Standard error is shown as
18 581 shaded grey.

19 582 **Figure 3.** Sub-daily responses of ecosystem evapotranspiration (ET_{eco}) and mountain
20 583 birch transpiration per unit leaf area (T_{leaf}) to PAR (panels a,c) and VPD (panels b,d),
21 584 measured at the corresponding ecological scale (i.e. ‘branch’ for T_{leaf} and ‘eco’ for
22 585 ET_{eco}) in Abisko (red) and Kevo (blue).

23 586 **Figure 4.** Response surfaces of modelled T_{leaf} (panels a, b) and ET_{eco} (panels c, d) as a
24 587 function of VPD and PAR, in Abisko (panels a, c) and Kevo (panels b, d). Please note
25 588 the different scales in the VPD axes in panels a and b compared to panels c and d.

26 589 **Figure 5.** Seasonal course of daily ecosystem evapotranspiration (ET_{eco} , black lines)
27 590 and upscaled birch transpiration (T_{birch} , grey lines), for Abisko (a) and Kevo (b). The
28 591 shaded regions in panels a and b depict upscaled T_{birch} using mean \pm SE values of LAI
29 592 (Table 1). Daily percentage of T_{birch}/ET_{eco} for Abisko (c) and Kevo (d). Panel (f) shows
30 593 evapotranspiration components and their upscaled values for Kevo only: ET_{eco} (black
31 594 line), T_{birch} (grey line), ET_{shrub} (purple line), ET_{lichen} (green line), $ET_{upscaled}$ (asterisk).

32 595 **Figure 6.** Variation of daily T_{birch} / ET_{eco} in response to VPD_{eco} (a), PAR_{eco} (b) and
33 596 SMD (c), for Abisko (red) and Kevo (blue). Models summary are shown in Table S3.

1
2
3
4
5
6
7
8
9
10
11
12
13
14
15
16
17
18
19
20
21
22
23
24
25
26
27
28
29
30
31
32
33
34
35
36
37
38
39
40
41
42
43
44
45
46
47
48
49
50
51
52
53
54
55
56
57
58
59
60

597 Significant interaction between site and environmental value is shown in solid line and
598 no-significant interaction in dashed line.

For Peer Review

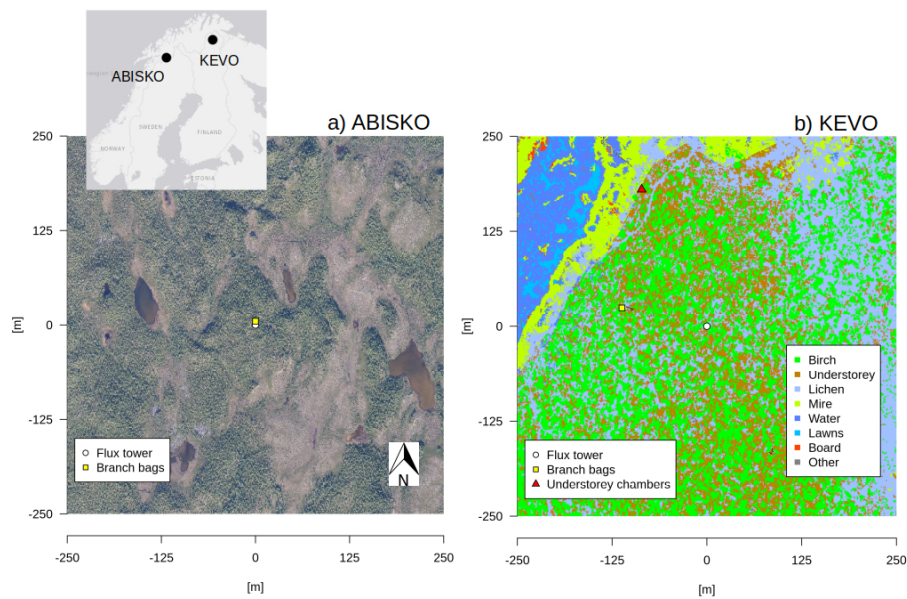


Figure 1. Study sites at Abisko (a) and Kevo (b), showing the locations of the branch bags systems, the eddy flux towers and the understorey automated chambers at Kevo. Panel (a) shows the aerial photography obtained in Abisko and (b) shows the land classification at Kevo obtained from aerial photography (cf. Hartley et al., 2015). Birch : mountain birch woodland; Understorey: low- and dwarf-shrubs; Lichen: lichen heath; Mire: organic hummocks and interhummocks with shrubs and Spahgnum; Water: open water; Lawns: graminoid lawns; Board: boardwalks; Other: other land cover.

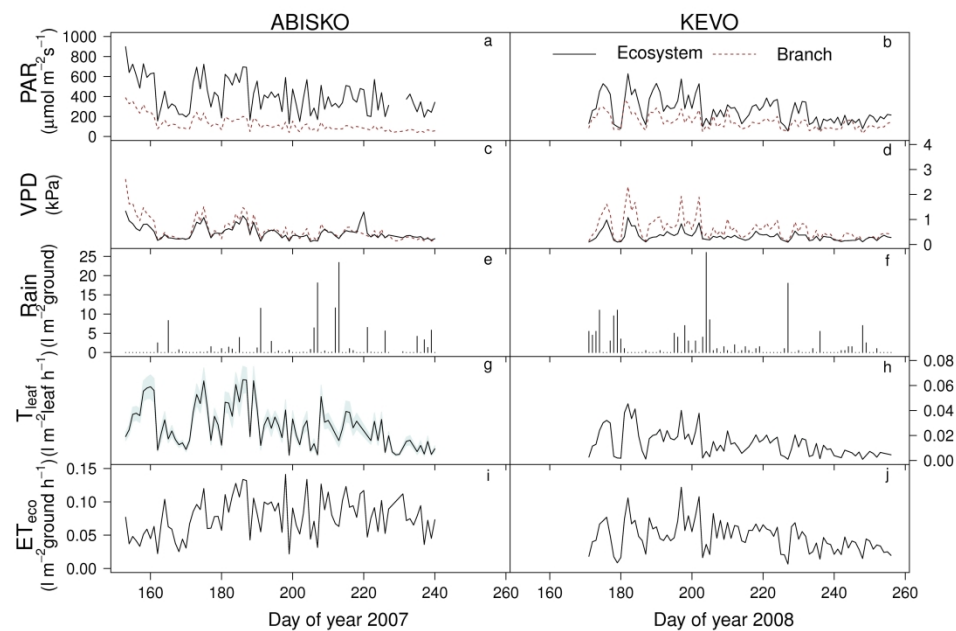


Figure 2. Seasonal course of environmental variables and evaporative fluxes (daily means) in Abisko and Kevo. Environmental variables include photosynthetically active radiation (a-b, PAR), vapour pressure deficit (c-d, VPD) and rainfall (e, f). Environmental variables were measured at the ecosystem (black lines) and at the branch level (red lines). Mountain birch transpiration per unit leaf area (g-h, T_{leaf}) and ecosystem evapotranspiration (i-j, ET_{eco}) are also shown. Standard error is shown as shaded grey.

359x242mm (300 x 300 DPI)

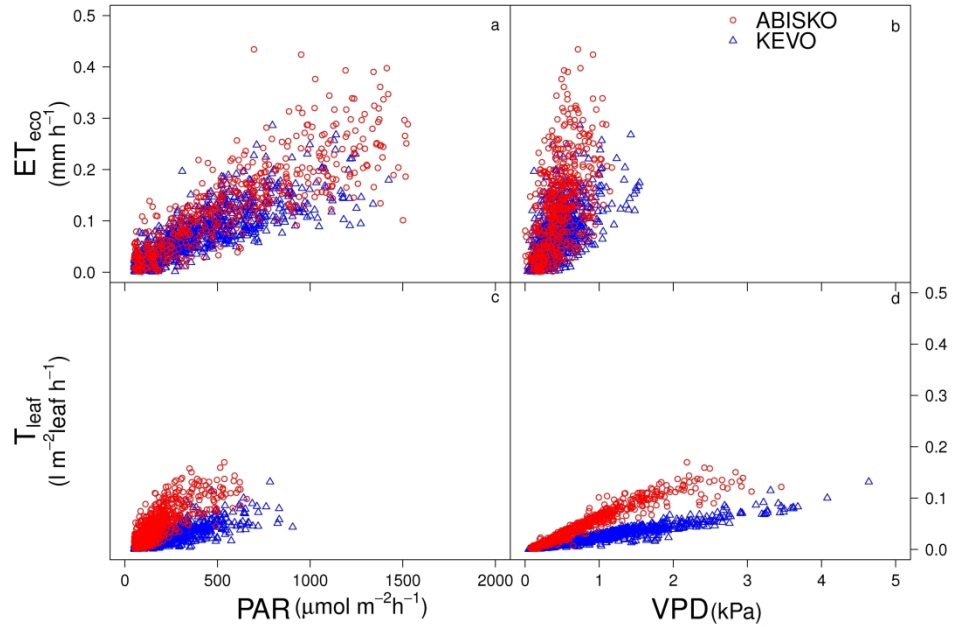


Figure 3. Sub-daily responses of ecosystem evapotranspiration (ET_{eco}) and mountain birch transpiration per unit leaf area (T_{leaf}) to PAR (panels a,c) and VPD (panels b,d), measured at the corresponding ecological scale (i.e. 'branch' for T_{leaf} and 'eco' for ET_{eco}) in Abisko (red) and Kevo (blue).

349x242mm (300 x 300 DPI)

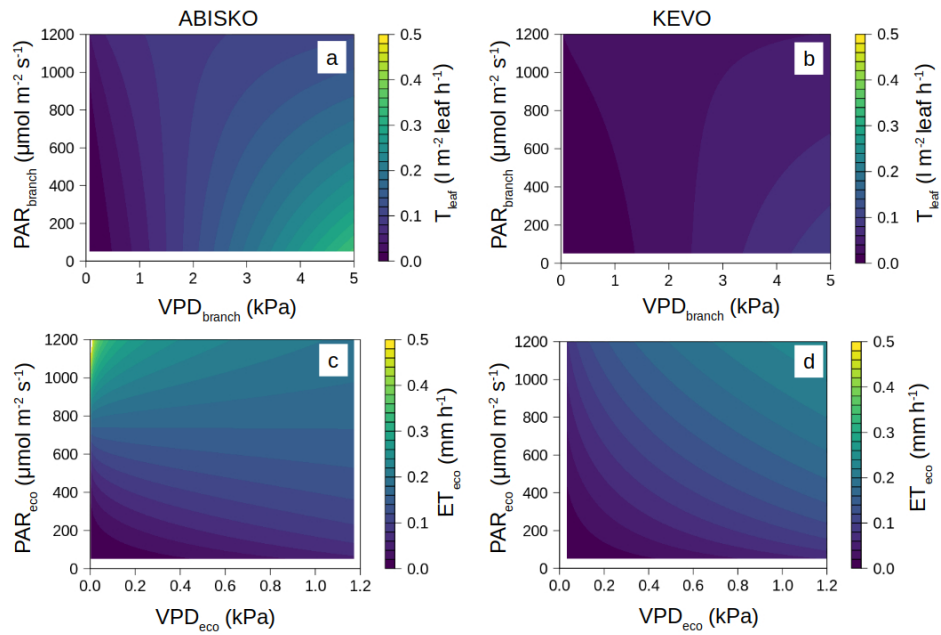


Figure 4. Response surfaces of modelled T_{leaf} (panels a, b) and ET_{eco} (panels c, d) as a function of VPD and PAR, in Abisko (panels a, c) and Kevo (panels b, d). Please note the different scales in the VPD axes in panels a and b compared to panels c and d.

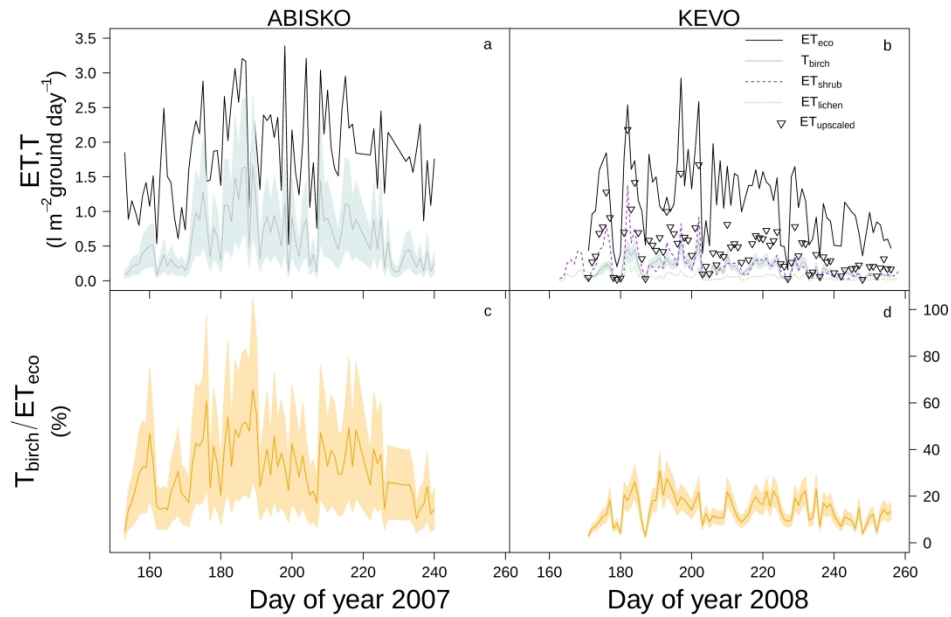


Figure 5. Seasonal course of daily ecosystem evapotranspiration (ET_{eco}, black lines) and upscaled birch transpiration (T_{birch}, grey lines), for Abisko (a) and Kevo (b). The shaded regions in panels a and b depict upscaled T_{birch} using mean ± SE values of LAI (Table 1). Daily percentage of T_{birch}/ET_{eco} for Abisko (c) and Kevo (d). Panel (f) shows evapotranspiration components and their upscaled values for Kevo only: ET_{eco} (black line), T_{birch} (grey line), ET_{shrub} (purple line), ET_{lichen} (green line), ET_{upscaled} (asterisk).

370x242mm (300 x 300 DPI)

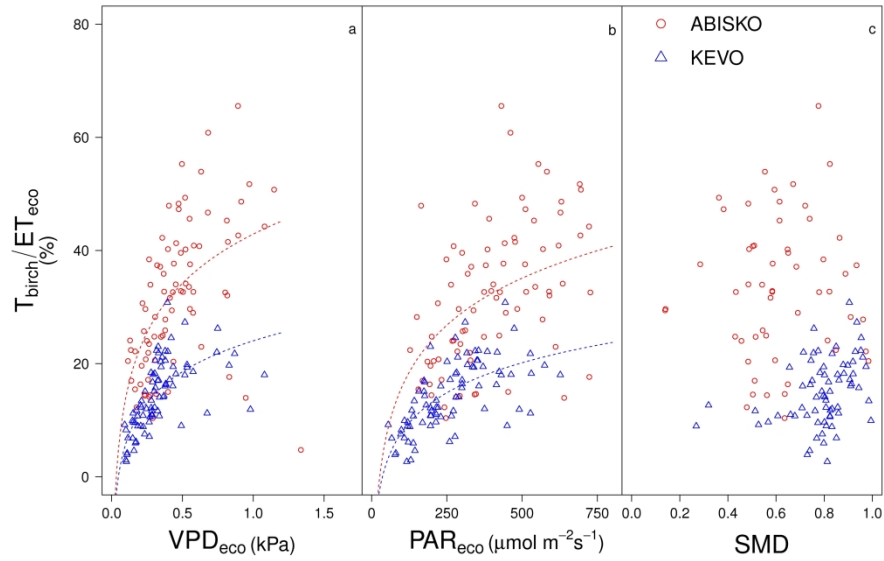


Figure 6. Variation of daily $T_{\text{birch}} / ET_{\text{eco}}$ in response to VPD_{eco} (a), PAR_{eco} (b) and SMD (c), for Abisko (red) and Kevo (blue). Models summary are shown in Table S3. Significant interaction between site and environmental value is shown in solid line and no-significant interaction in dashed line.

396x242mm (300 x 300 DPI)

1 **Supporting Information**

2 **S1. Allometric relationships**

3 **Table S1.** Summary statistics for the allometric relationships used to predict leaf area
4 supported by individual stems in Abisko and Kevo. Intercepts are labelled as a and
5 coefficients associated to the different predictors are labelled as b_i .

Site	Response [units]	a	SE	Predictor [units]	b_i	SE	R^2_{adj}
Abisko	ln(leaf biomass) [kg]	-8.11	0.71	ln (stem basal area) [mm ²]	0.43	0.11	0.86
				ln (stem height) [dm]	1.06	0.37	
Kevo	ln (leaf biomass) [g]	-4.95	0.25	ln (stem diameter) [mm]	1.56	0.07	0.97

6
7 In Kevo, trees frequently presented a number of small stems (DBH<12mm), whose
8 number was recorded in the forest inventories; there were *ca.* 876 small stems ha⁻¹. To
9 account for the leaf area supported by these stems, we assumed a typical diameter of 6
10 mm (half the value of the DBH threshold in the inventory) for these stems and applied
11 the allometric relationship above. Leaf area of small stems amounted, on average, 5% of
12 total plot leaf area.

13 **S2. Technical description of the branch bags system**

14 Branch bags (average volume=0.11 m³) were hung from tripods and poles to enclose the
15 sampled branches. A data-logger (CR10X, Campbell Scientific UK, Shepshed,
16 Leicester, UK) and a control interface (SDM-CD16AC, Campbell Scientific UK)
17 controlled which bag was being sampled by delivering power to the electromagnetic
18 catch that sealed the bag, the internal mixing fan and the corresponding diaphragm
19 pump. This pump sampled air from the bag (5 dm³ min⁻¹) through polyethylene-lined
20 tubing, 5 mm in diameter, to an enclosure where a solenoid and another pump diverted
21 the air sample (0.2 dm³ min⁻¹) to an IRGA (LI-6262, LICOR Inc., Lincoln NE, USA).

22 All the sampled branches were within *ca.* 10 m from this control box. Outputs from all
 23 sensors and IRGA were transmitted through a relay multiplexer (AM416, Campbell
 24 Scientific UK) and stored in the data-logger.

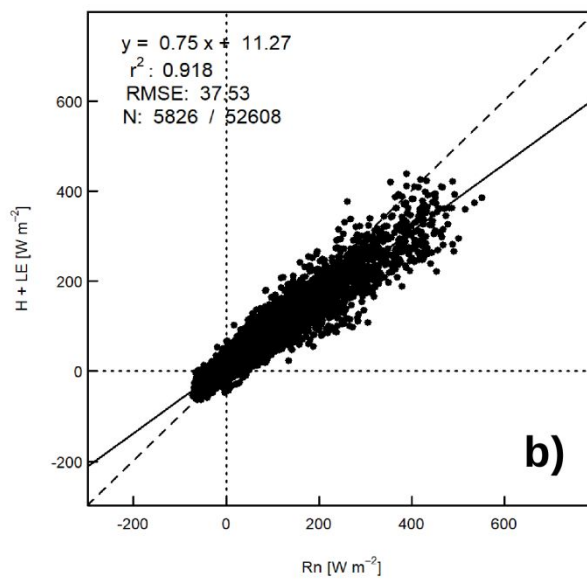
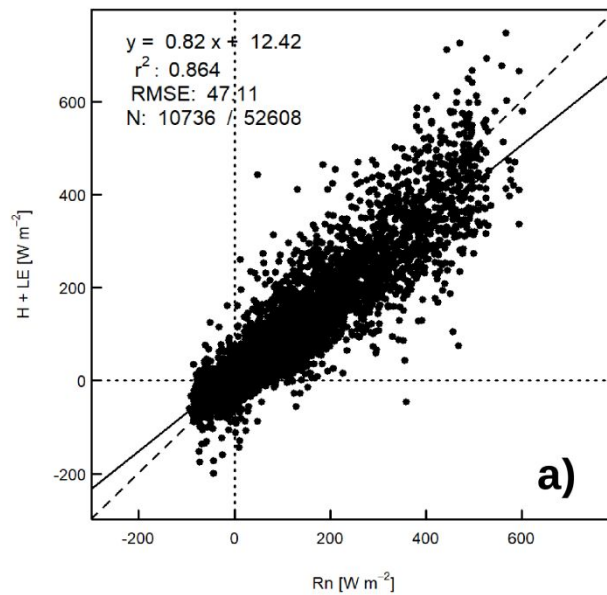
25 Each bag remained closed for 7.5 minutes (completing a measurement cycle of the eight
 26 branches in one hour), during which H₂O concentrations were measured every 5 s. with
 27 the IRGA operating in absolute mode. Air temperature, relative humidity (HMP45C,
 28 Vaisala, Vantaa, Finland), and air pressure (LI-6262-03, LI-COR Inc.) were also
 29 recorded every 5 s. Average Photosynthetically Active Radiation (PAR) was also
 30 measured inside the branch bags (SD101QV/SD201QV, Macam Ltd., Livingston, UK).

31 We calculated branch transpiration within the branch bag, T_{branch} (mmol s⁻¹), as:

$$32 E_{branch} = \frac{P_{bag} V_{bag}}{RT_{bag,0}} \frac{d[H_2O]_{bag}}{dt} \quad (\text{Eq. S1})$$

33 Where P_{bag} (Pa) is air pressure, V_{bag} (m³) is bag volume, R (J mol⁻¹ K⁻¹) is the ideal gas
 34 constant, $T_{bag,0}$ (K) is absolute temperature inside the bag and $d[H_2O]_{bag}/dt$ (mmol s⁻¹) is
 35 the rate of change in H₂O vapour concentration (mmol) during each observation. The
 36 $d[H_2O]_{bag}/dt$ (mmol s⁻¹) was estimated from the first order term of a quadratic fit
 37 between H₂O vapour concentration (mmol) and time since chamber closure (Poyatos,
 38 Gornall, Mencuccini, Huntley, & Baxter, 2012). Nonlinear fits describe better the
 39 concentration dynamics, and do not systematically underestimate the fluxes (Wagner,
 40 Reicosky, & Alessi, 1997). However, in the presence of noisy concentration data under
 41 low flux conditions, we opted for the more stable linear fit. We achieved this by
 42 selecting the linear regression whenever the slope for the linear fit and the linear term of
 43 the quadratic fit had opposite signs. Flux calculations were implemented in a R script (v
 44 2.9, R Development Core Team, Vienna, Austria), which also included tests for
 45 autocorrelation (Durbin-Watson) and normality (Shapiro-Wilk) of residuals for each
 46 flux observation (Kutzbach et al., 2007), and produced diagnostic plots of
 47 instantaneous H₂O concentrations during each observation. The values of T_{branch} were
 48 transformed from molar to volume using the molar volume of water and converted to
 49 hourly rates (l hour⁻¹), prior to their conversion to transpiration per unit leaf area T_{leaf}
 50 (cf. main text).

51

52 **S3. Energy balance closure in eddy covariance measurements**

53

54 **Figure S1.** The sum of sensible and latent heat fluxes versus net radiation (ground heat
55 flux and heat stored in the canopy are neglected) in Abisko (a) and Kevo (b).

3

For Peer Review

57 **S4. Data temporal aggregation and gap-filling**

58 Due to technical problems of the measurement systems, gaps in temporal series were
 59 present. Not accounting for these gaps could bias the quantification of daily and
 60 seasonal aggregates of evaporative fluxes. To address this, hourly T_{leaf} and ET_{eco} were
 61 gap-filled with values predicted by the models presented in the main text (Table 2, 3).
 62 Gap-filling of ET_{shrub} and ET_{lichen} were performed using a similar modelling strategy,
 63 using PAR and VPD as predictors. The models for these two hourly fluxes showed a
 64 marginal and conditional R^2 of 0.54 and 0.56, respectively. However, we could not
 65 make predictions when meteorological variables were also missing. Therefore, daily
 66 aggregates of T_{leaf} were calculated when data for at least three branches and 50% of
 67 hours in each day were present; the same criterion for the minimum number of
 68 timesteps was applied for ET_{eco} and for environmental drivers such as PAR and VPD.
 69 Precipitation was calculated as the daily summation of hourly values. After this hourly
 70 gap-filling, days with missing data were imputed using daily models of the
 71 corresponding evaporative flux and its drivers. When drivers (VPD, PAR) were also
 72 missing, we gap-filled these data using data from nearby sensors deployed within the
 73 ABACUS measuring campaigns. The overall number of hourly gaps across the growing
 74 season was overall very low for the branch bags system, and higher for the eddy
 75 covariance and the understorey chambers and the R^2 of the daily models ranged
 76 between 0.7 and 0.8 (Table S2).

77 **Table S2.** Percentage of hourly gaps that had to be imputed using hourly or daily
 78 models of evaporative fluxes as a function of VPD and PAR. The R^2 of daily models is
 79 also shown.

	% of hourly gaps	Daily model R^2
Abisko		
T_{birch}	6%	Not needed
ET_{eco}	37%	0.70
Kevo		
T_{birch}	6%	0.79

ET _{eco}	25%	0.80
ET _{lichen}	44%	0.69
ET _{shrub}	42%	0.69

80

81 **S5. Technical description of the automated chamber system for measuring tundra**
 82 **evapotranspiration**

83 In Kevo, at *ca.* 150 m from the eddy flux tower, we deployed 12 PVC collars (19.9 cm
 84 internal diameter and 4.5 cm height) in early June 2008 to measure four microsite types
 85 of tundra communities, with three replicates for each type (cf. Table 1 in Poyatos et al.
 86 2014). Three microsite types were dominated by tundra shrubs and differed in their
 87 spatial location, both in terms of microtopography and position along the mire to forest
 88 ecotone (Poyatos et al., 2014).

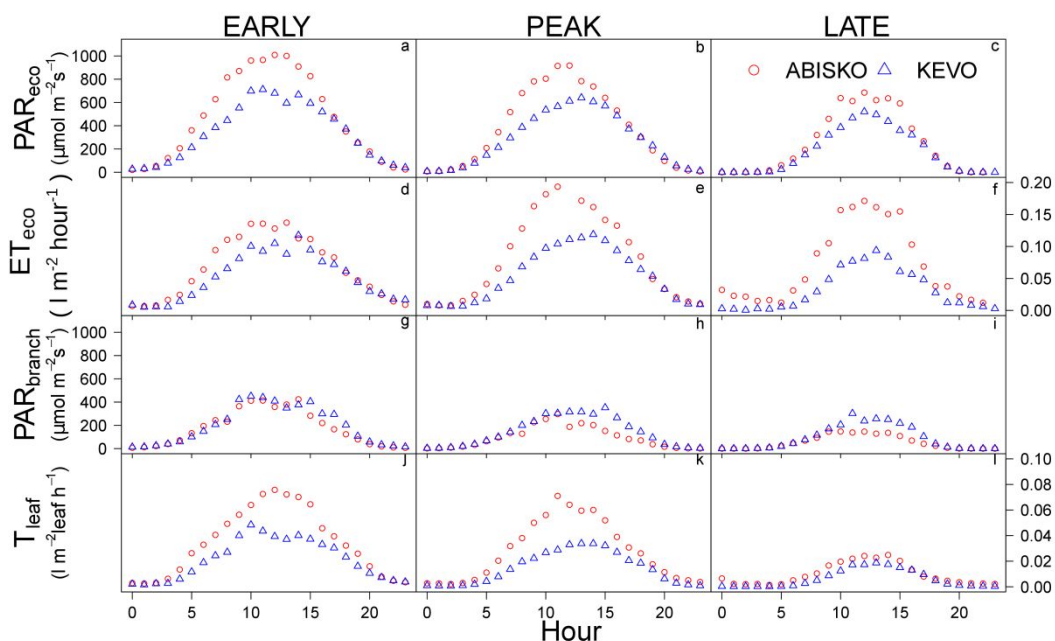
89 We used a closed dynamic gas exchange system for measuring H₂O flux rates (mmol
 90 H₂O m⁻² s⁻¹). The system comprised an infra-red gas analyser (Li-Cor 8100, Li-Cor Inc.,
 91 Lincoln, Nebraska, USA), a custom-built multiplexed gas handler unit (Electronics
 92 Workshop, Biology Department, University of York, UK) and 12 clear, Perspex
 93 chambers based on a commercial soil respiration model (LiCor 8100-101; 20 cm
 94 diameter). Chambers closed and opened sequentially, allowing hourly measurement
 95 cycles of 12 vegetation patches at a maximum radial distance of 20 m from the
 96 multiplexer. The chamber bases had rims with a rubber gasket, which ensured a tight fit
 97 with PVC collars. These collars were deployed on the 12 selected patches and gently
 98 sealed to the ground, without cutting or inserting into the substrate, using non-setting
 99 plumber's putty (Plumber's Mait, Bostik Ltd., Leicester, UK). We took this precaution
 100 to avoid damaging the prostrate stems and the roots of dwarf-shrub tundra species,
 101 which could potentially affect measured fluxes. The system operated from the 11th of
 102 June (DOY 163) until the 14th of September (DOY 258) of 2008.

103 Evapotranspiration from the chamber $ET_{chamber}$ (mmol H₂O m⁻² s⁻¹) was calculated as:

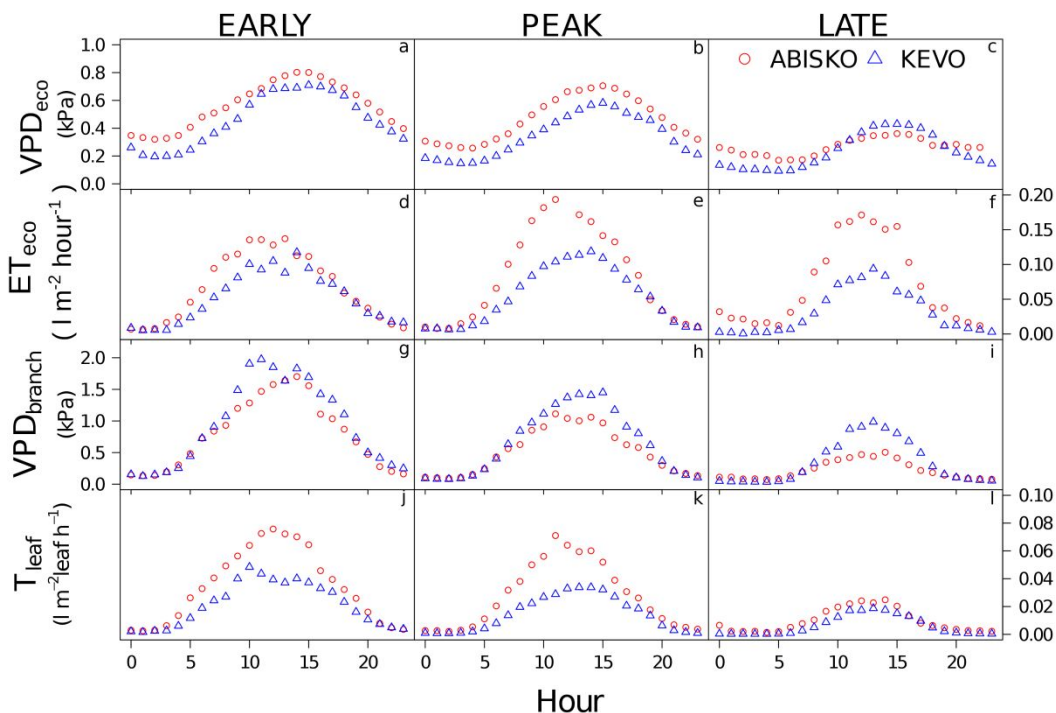
$$104 \quad ET_{chamber} = \frac{P_{chamber} V_{chamber}}{RT_{chamber,0}} \frac{d[H_2O]_{chamber}}{dt} \quad (\text{Eq.S2})$$

1
2
3 105 where $P_{chamber}$ is air pressure inside the chamber (Pa), $V_{chamber}$ (m^3) is the system volume
4
5 106 (chamber, irga/multiplexer and tubing), $T_{chamber,0}$ ($^{\circ}C$) is air temperature at chamber
6
7 107 closure, R ($J K^{-1} mmol^{-1}$) is the ideal gas constant, $A_{chamber}$ is chamber surface area (m^2)
8
9 108 and $d[H_2O]/dt$ ($mmol mol^{-2}s^{-1}$) is the rate of change in water vapour in the chamber
10
11 109 headspace. We calculated this rate from water vapour concentrations measured every 2
12
13 110 seconds, over the 150 s period when the chamber remained closed. We estimated
14
15 111 $d[H_2O]/dt$ from the first order term of a quadratic fit between $[H_2O]$ and time since
16
17 112 chamber closure. Nonlinear fits describe better the concentration dynamics in the closed
18
19 113 chamber, and do not systematically underestimate the fluxes. However, in the presence
20
21 114 of noisy concentration data under low flux conditions, we opted for the more stable
22
23 115 linear fit; we selected the linear regression whenever the slope for the linear fit and the
24
25 116 linear term of the quadratic fit had opposite signs (cf. Supporting Information
26
27 117 S2). Because of microclimatic alterations, water vapour sorption in the tubing system
28
29 118 and imperfect chamber sealing the automated chamber system used here has been
30
31 119 reported to underestimates the evaporative fluxes (Cohen et al., 2015). Therefore, we
32
33 120 applied a correction factor of *ca.* 2.3, obtained in this latter study, which used a similar
34
35 121 device under comparable environmental conditions (Cohen et al., 2015).
36
37
38
39
40
41
42
43
44
45
46
47
48
49
50
51
52
53
54
55
56
57
58
59
60

122

123 **S6. Seasonal variation in the daily patterns of evaporative fluxes**

124 **Figure S2.** Seasonal variation in the mean daily patterns of ecosystem
 125 evapotranspiration (ET_{eco}) and birch transpiration per unit leaf area (T_{leaf}) compared to
 126 mean daily variation in PAR at the corresponding measurement scale. The growing
 127 season was split into three distinct periods according to leaf phenology (Early: 153-185,
 128 171-185; Peak: 186-225, 186-230; Late: 226-241, 231-257, DOY in Abisko and Kevo,
 129 respectively).



1
2
3
4
5
6
7
8
9
10
11
12
13
14
15
16
17
18
19
20
21
22
23
24
25
26
27
28
29
30
31
32
33
34
35
36
37
38
39
40
41
42
43
44
45
46
47
48
49
50
51
52
53
54
55
56
57
58
59
60

130 **Figure S3.** Seasonal variation in the mean daily patterns of ecosystem
131 evapotranspiration (ET_{eco}) and birch transpiration per unit leaf area (T_{leaf}) compared to
132 mean daily variation in VPD at the corresponding measurement scale. The growing
133 season was split into three distinct periods according to leaf phenology (Early: 153-185,
134 171-185; Peak: 186-225, 186-230; Late: 226-241, 231-257, DOY in Abisko and Kevo,
135 respectively).

136

137 **S7. Footprint modeling**

138 The contribution of different land cover types to the eddy covariance source area was
139 estimated using an analytical footprint model (Hsieh, Katul, & Chi, 2000) assuming
140 lateral dispersion (Detto, Montaldo, Albertson, Mancini, & Katul, 2006; Schmid, 1994).
141 To save computation time a look-up-table approach was used (Crawford, Grimmond,
142 Ward, Morrison, & Kotthaus, 2017), where the observed meteorological conditions at
143 each 30-min timestep were matched to the pre-calculated land cover composition.
144 Intervals of 15° , 0.2 m s^{-1} and 0.5 m s^{-1} were used for wind direction, friction velocity,
145 and standard deviation of lateral wind, respectively; and three stability classes
146 accounted for stable, unstable and neutral conditions. Typically, more than 80% of the
147 source area was located within 500 m of the tower, with the peak contribution at a
148 distance of about 23 m (36 m) in unstable (stable) conditions. As the land cover around
149 the tower is a mixture of lichen, shrubs and birch, the variation in footprint composition
150 with atmospheric conditions is small. (e.g. there is a slightly larger contribution from
151 lichen for northeasterly winds and from trees for southwesterly winds, and the
152 contribution of graminoid lawns and vascular plants near water is greater under stable
153 conditions than unstable conditions).

154 The average footprint composition for the study period (DOY 160-260) is shown in
155 Table S2 (percentage contributions have been scaled to give a total of 100%). Trees
156 form the largest contribution (40%), followed by understorey (29%), followed closely
157 by lichen (25%), with other land cover types contributing only a few percent at most.

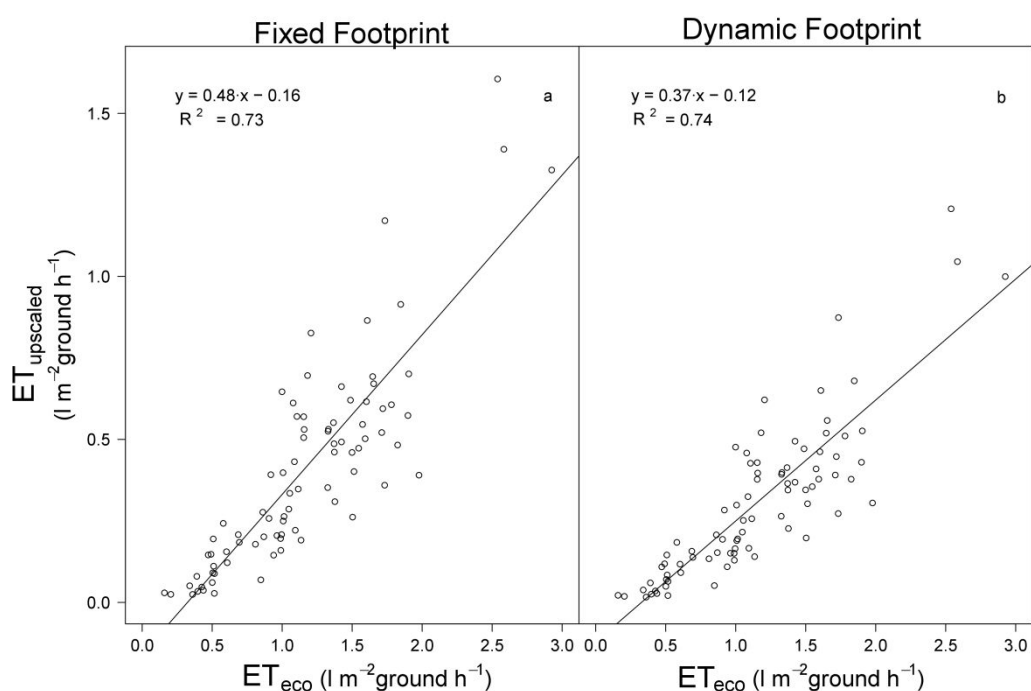
158

159

160 **Table S3:** Average footprint composition for the study period in Kevo.

Land cover type	Average contribution to footprint [%]
Lichen	25.1
Vascular plants near water	3.4
Graminoid lawns	2.3
Understorey	29.1
Sphagnum	< 0.1
Trees	39.6
Road, boardwalk, powerlines	0.1
Open water	0.5

161

162 **S8. Evapotranspiration upscaling using fixed and dynamic footprint**

163

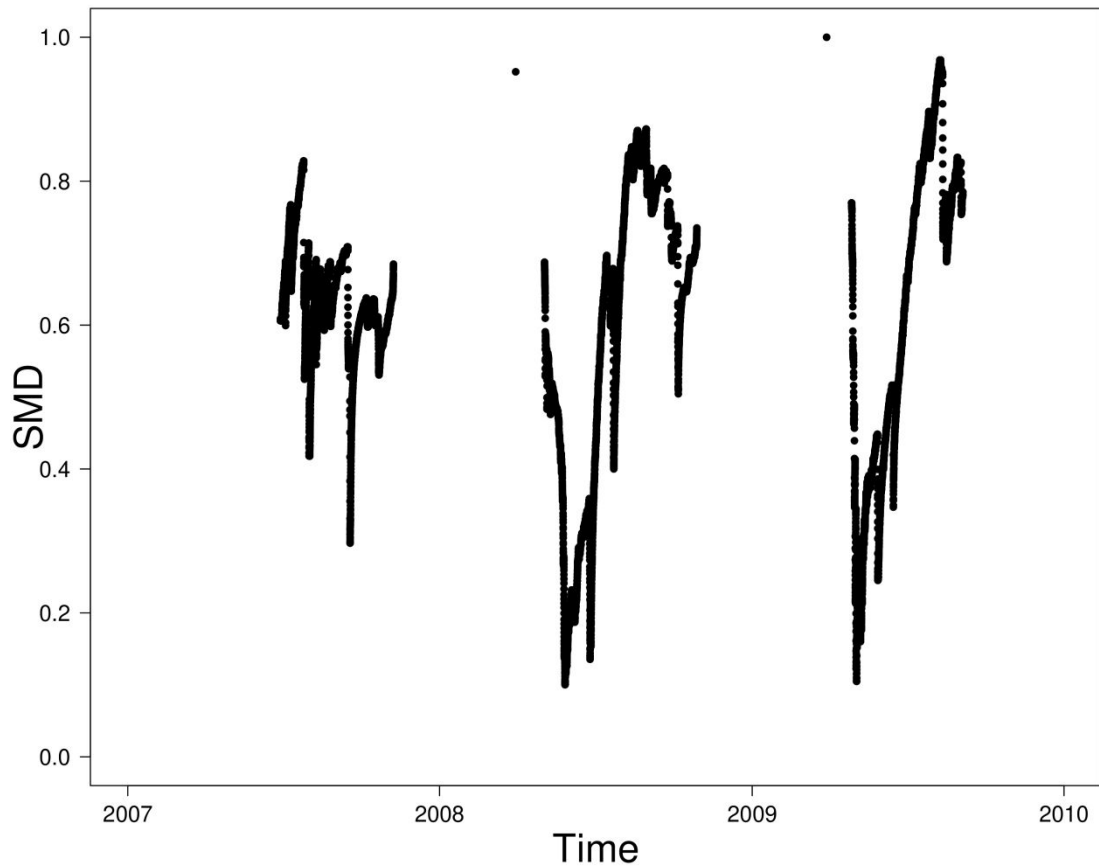
164 **Figure S4.** Linear regressions between ET_{eco} and $ET_{upscaled}$ using a fixed (a) or (b)
165 dynamic footprint approach.

166

167 **S9. Variation of daily T_{birch}/ET_{eco} in response to VPD_{eco} , PAR_{eco} and SMD.**

168 **Table S4.** Linear models of T_{birch}/ET_{eco} in response to VPD, PAR and SMD after
 169 applying AIC-based model selection (cf. Methods). The reference level in this model is
 170 Abisko and significance codes are: * $p < 0.05$, ** $p < 0.01$, *** $p < 0.001$.

VPD model				
	Estimate	SE	t-value	p
(Intercept)	42.896	1.781	24.079	$< 2 \cdot 10^{-16}$ ***
log(VPD)	12.554	1.689	7.432	$6.19 \cdot 10^{-12}$ ***
siteKevo	-18.863	2.890	-6.527	$8.56 \cdot 10^{-10}$ ***
log(VPD) : siteKevo	-4.661	2.390	-1.950	0.053
PAR model				
	Estimate	SE	t-value	p
(Intercept)	-39.354	13.191	-2.984	0.0033 **
log(PAR)	11.981	2.223	5.391	$2.5 \cdot 10^{-7}$ ***
siteKevo	12.023	16.555	0.726	0.469
Log(PAR) : siteKevo	-4.340	2.887	-1.508	0.133
SMD model				
	Estimate	SE	t-value	p
(Intercept)	33.435	1.256	26.62	$< 2 \cdot 10^{-16}$ ***
siteKevo	-18.454	1.679	-10.99	$< 2 \cdot 10^{-16}$ ***



175 **S10. Soil moisture deficit dynamics in Abisko in 2007 - 2009**

176 **Figure. S5.** Soil moisture deficit (SMD) in Abisko in 2007 – 2009 showing the
177 continuous increase after snowmelt in 2008 and 2009.

178

179 **References**

- Cohen, L. R., Raz-Yaseef, N., Curtis, J. B., Young, J. M., Rahn, T. A., Wilson, C. J., ... Newman, B. D. (2015). Measuring diurnal cycles of evapotranspiration in the Arctic with an automated chamber system. *Ecohydrology*, 8(4), 652–659. <https://doi.org/10.1002/eco.1532>
- Crawford, B., Grimmond, C. S. B., Ward, H. C., Morrison, W., & Kotthaus, S. (2017). Spatial and temporal patterns of surface–atmosphere energy exchange in a dense urban environment using scintillometry. *Quarterly Journal of the Royal Meteorological Society*, 143(703), 817–833. <https://doi.org/10.1002/qj.2967>
- Detto, M., Montaldo, N., Albertson, J. D., Mancini, M., & Katul, G. (2006). Soil moisture and vegetation controls on evapotranspiration in a heterogeneous Mediterranean ecosystem on Sardinia, Italy. *Water Resources Research*, 42(8). <https://doi.org/10.1029/2005WR004693>
- Hsieh, C.-I., Katul, G., & Chi, T. (2000). An approximate analytical model for footprint estimation of scalar fluxes in thermally stratified atmospheric flows. *Advances in Water Resources*, 23(7), 765–772. [https://doi.org/10.1016/S0309-1708\(99\)00042-1](https://doi.org/10.1016/S0309-1708(99)00042-1)
- Kutzbach, L., Schneider, J., Sachs, T., Giebels, M., Nykanen, H., Shurpali, N. J., ... Wilmking, M. (2007). CO₂ flux determination by closed-chamber methods can be seriously biased by inappropriate application of linear regression. *Biogeosciences*, 4(6), 1005–1025.
- Poyatos, R., Gornall, J., Mencuccini, M., Huntley, B., & Baxter, R. (2012). Seasonal controls on net branch CO₂ assimilation in sub-Arctic Mountain Birch (*Betula pubescens* ssp. *Czerepanovii* (Orlova) Hamet-Ahti). *Agricultural and Forest Meteorology*, 158–159, 90–100. <https://doi.org/10.1016/j.agrformet.2012.02.009>
- Poyatos, R., Heinemeyer, A., Ineson, P., Evans, J. G., Ward, H. C., Huntley, B., & Baxter, R. (2014). Environmental and Vegetation Drivers of Seasonal CO₂ Fluxes in a Sub-arctic Forest–Mire Ecotone. *Ecosystems*, 17(3), 377–393. <https://doi.org/10.1007/s10021-013-9728-2>
- Schmid, H. P. (1994). Source areas for scalars and scalar fluxes. *Boundary-Layer Meteorology*, 67(3), 293–318. <https://doi.org/10.1007/BF00713146>
- Wagner, S. W., Reicosky, D. C., & Alessi, R. S. (1997). Regression models for calculating gas fluxes measured with a closed chamber. *Agronomy Journal*, 89(2), 279–284.

180